The explosive radiation of the Neotropical *Tillandsia* subgenus *Tillandsia* (Bromeliaceae) has been facilitated by pervasive hybridization

Gil Yardeni[1,2] , Michael H. J. Barfuss[1], Walter Till[1], Matthew R. Thornton[1], Clara Groot Crego[1,3], Christian Lexer[1,§], Thibault Leroy[1,4,*], Ovidiu Paun[1,*]

[1]*Department of Botany and Biodiversity Research, University of Vienna, Vienna, Austria*

[2]*Institute of Computational Biology, Department of Biotechnology, University of Life Sciences and Natural Resources, Vienna, Austria.*

[3]*Vienna Graduate School of Population Genetics, Vienna, Austria*

[4]*GenPhySE, Université de Toulouse, INRAE, ENVT, Castanet Tolosan, France*

[§]*deceased*

**shared last authorship*

Corresponding authors: gil.c.yardei@gmail.com; ovidiu.paun@univie.ac.at

Abstract

The recent rapid radiation of *Tillandsia* subgenus *Tillandsia* (Bromeliaceae) provides an attractive system to study the drivers and limits of species diversification. This species-rich Neotropical monocot clade includes predominantly epiphytic species displaying vast phenotypic diversity. Recent in-depth phylogenomic work revealed that the subgenus originated within the last 7 MY while expanding through one major event from South into Central America within the last 5 MY. However, disagreements between phylogenies and lack of resolution at shallow nodes suggested that hybridization occurred throughout the radiation, together with frequent incomplete lineage sorting and/or considerable gene family evolution. We used whole-genome resequencing data and a newly available reference genome to explore the evolutionary history of 34 representative ingroup species employing both a tree-based and a network approach. Our results indicate that lineage co-occurrence does not predict relatedness and confirm significant deviations from a tree-like structure, coupled with pervasive gene tree discordance. Focusing on hybridization, ABBA-BABA and related statistics were used to infer the rates and relative timing of introgression, while topology weighting uncovered high heterogeneity of the phylogenetic signal along the genome. High rates of hybridization within and among clades suggest that, in contrast to previous hypotheses, the expansion of subgenus *Tillandsia* into Central America proceeded in several dispersal events, punctuated by episodes of diversification and gene flow. Network analysis revealed reticulation as a prominent propeller during radiation and establishment in different ecological niches. This work contributes a plant example of prevalent hybridization

during rapid species diversification, supporting the hypothesis that interspecific gene flow facilitates explosive diversification.

Keywords: *Tillandsia*, gene tree discordance, hybridization, phylogenomics, bromeliad, Neotropical diversity, species network

Rapid evolutionary radiations are characterised by accelerated and substantial diversification, usually following dispersal into a novel geographic area. As a myriad of diverse ecological spaces become available, a lineage can opportunistically adapt to quickly occupy them in a process termed adaptive radiation (Hughes et al. 2015; Linder 2008; Naciri and Linder 2020; Rundell and Price 2009; Stroud and Losos 2016). Rapid radiations provide ample opportunities to investigate the mechanisms driving diversification. While not all rapid radiations are adaptive, i.e., not necessarily associated with an increase in ecological occupancy (Givnish 2015; Schluter 2000; Stroud and Losos 2016), evolutionary radiations are generally connected with habitat heterogeneity (Paun et al. 2016; Soltis et al. 2019), climatic fluctuations (Slovak et al. 2023), landscape fragmentation (Hughes and Atchison 2015) and/or orogenesis (Boschman and Condamine 2022). Ubiquitous among angiosperms in general and in the Neotropics in particular, plant radiations remain to date understudied and enigmatic, especially when compared to animal systems (but see e.g., Drummond et al. 2012; Lagomarsino et al. 2016; Linder 2008; Paun et al. 2016; Pérez-Escobar et al. 2017; Richardson et al. 2001).

Phylogenomic studies of young rapid radiations must overcome multiple challenges, as low sequence divergence and incomplete reproductive barriers increase the probability of short internal branches and impede phylogenomic resolution (Giarla and Esselstyn 2015; Straub et al. 2014; Whitfield and Lockhart 2007). Frequent shifts at key traits can be distinctly associated with phylogenetic conflict, stemming from population-level processes like changes in population size, incomplete lineage sorting (ILS) and reticulation (Oliver 2013; Parins-Fukuchi et al. 2021). Such processes were traditionally deemed as analytical noise when aiming to reconstruct bifurcating species trees. Yet an increasing amount of

research indicates that episodes of phylogenomic conflict represent typical signatures of microevolutionary processes during rapid species diversification (Filiault et al. 2018; Parins-Fukuchi et al. 2021). Hence, gene-tree conflict and non-bifurcating relationships should be viewed and studied as defining features of diversification processes during rapid radiations (Malinsky et al. 2018; Slovak et al. 2023; Wogan et al. 2023).

Introgression has recently emerged as a key driver of species' diversification (e.g. Abbott et al. 2013; Seehausen 2004) with gene flow regarded as an important process during speciation (Barth et al. 2020; Linck and Battey 2019; Mallet et al. 2016). Gene flow between recently diverged species is thought to increase their genetic variability and enrich the genomic substrate for natural selection to act on. Interspecific hybridization can prompt ecological diversification through heterosis and adaptive introgression, a process in which advantageous alleles are incorporated in new genomic backgrounds from one gene pool to another. Furthermore, introgression can introduce advantageous alleles upon which selection has already acted, thus catalysing evolutionary radiations (Abbott et al. 2013; Edelman et al. 2019; Harrison and Larson 2014; Meier et al. 2019; Suarez-Gonzalez et al. 2018).

The rapidly radiating and highly diverse Neotropical *Tillandsia* subg. *Tillandsia* provides a particularly relevant study system to investigate the drivers of radiations. Subgenus *Tillandsia* is the most diverse of seven subgenera within genus *Tillandsia* (family Bromeliaceae). It consists of more than 250 species of predominantly epiphytic plants, distributed from southeastern United States to central Argentina (Barfuss et al. 2016). Members of the subgenus exhibit tremendous morphological diversity of adaptive traits which allows them to occupy disparate habitats, from tropical rainforests to deserts, and from low- to highlands (Benzing 2000; Givnish et al. 2011). Adaptations such as adventitious

roots, trichomes modified for water and nutrient absorption, a water-impounding leaf rosette tank and Crassulacean acid metabolism (CAM) appear to have undergone in some cases correlated and in others contingent evolution, resulting in adaptive syndromes (Givnish et al. 2014). Early efforts employing conserved plastid and nuclear markers recovered largely inconsistent phylogenetic relationships within the subgenus (Barfuss et al. 2005; 2016; Chew et al. 2010; Granados Mendoza et al. 2017; Pinzón et al. 2016). Using plastome phylogenomics, Vera-Paz et al. (2023) confirmed the monophyly of the subgenus and the presence of three main clades within the subgenus, including a monophyletic, radiated 'clade K' with members distinctly distributed in North and Central America (Barfuss et al. 2016; Granados Mendoza et al. 2017). They further identified clades K.1 and K.2 as subclades of clade K which we have further renamed to reflect phylogenetic groups (see Methods; Supporting Table S1). Several studies (Givnish et al. 2014; Till 2000; Vera-Paz et al. 2023; Winkler, 1990) discussed that the ancestor of 'clade K' was most likely South American and expanded to Central America approximately 4.9 Mya, and subsequently dispersed multiple times to North America. However, the relationships within the clade remained elusive and disagreements between gene trees are common, calling to consider the role of different evolutionary processes in the *Tillandsia* radiation. As a result, hybridization was put forward as especially prevalent in the subgenus (Till 2000; Vera-Paz et al. 2023).

Using whole-genome resequencing data and a newly available reference genome, our study aims to shed light on the evolutionary history of the radiation of *Tillandsia* subgenus *Tillandsia*, focusing on Central American groups within the radiated 'clade K' and representatives of South American species. Specifically, our objectives are to infer relationships between representative species and investigate the signals of phylogenetic

conflict, with a ultimate aim to characterise and quantify hybridization and gene-flow. Additionally, we highlight patterns of gene-flow which may have contributed to adaptive trait shift in this Neotropical rapid radiation. Our detailed analyses provide evidence of a deeply reticulated history within the subgenus and of at least two colonisation events from South into Central America, surprisingly refuting the monophyly of the so-called ‘clade K’.

Materials and Methods

Plant Material Collection

Leaf material was collected from 69 individuals belonging to 37 *Tillandsia* species. Material from field collections was cut lengthwise and immediately dried in powdered silica gel. Samples from the botanical collection of the University of Vienna were extracted fresh (Supporting Tables S1, S3). 69 accessions correspond to 34 species of *Tillandsia* subg. *Tillandsia*, while the remaining two belong to subg. *Allardtia* sensu Smith & Downs (1977) and were used as outgroups. Of the 34 ingroup species, 26 represent the Central-North American 'clade K' radiation and eight species represent South American *Tillandsia* (henceforth: SA clades; Supporting Fig. 1, Supporting Table S1). Albeit not exhaustive, our sampling was performed with the intention to represent the variety of morphological and physiological syndromes within clades SA and 'K' (Supporting Table S2). Species in 'clade K' are mostly epiphytic and ornithophilous, whereas clade SA includes epiphytic, saxicolous and tank forming xerophitic species, predominantly endemic to Peru (with the exception of *Tillandsia adpressiflora*; Supporting Tables S1-2). The *T. fasciculata* clade (previously K.2.3) includes species largely exhibiting CAM photosynthetic syndrome with typical water-absorbing trichomes. In addition, species within this clade present varying distributions, from endemic to widespread, some extending into the Antilles. The *T. guatemalensis* clade (previously K.2.2) is a small group of widespread and predominantly-C3 plants, exhibiting smooth leaves and a prominent tank habit. The *T. punctulata* (K.1) and *T. utriculata* (K.2.1) clades include widespread or endemic species with intermediate CAM-C3 syndromes or various CAM-like photosynthetic syndromes, respectively.

DNA Library Preparation

DNA extractions were performed as previously described (Yardeni et al. 2022) using a modified CTAB protocol (Doyle and Doyle, 1987) or the QIAGEN DNeasy® Plant Mini Kit (Qiagen, USA). They have been further purified using the Nucleospin® gDNA cleanup kit from Macherey-Nagel (Hudlow et al. 2011). The extracts were subsequently diluted in water and quantified with a Qubit® 3.0 Fluorometer (Life Technologies, Carlsbad, CA, USA). Prior to library preparation, a maximum of 600 ng of DNA per accession was sheared at 4°C to a target average length of 400 bp using a Bioruptor® Pico sonication device (Diagenode, Denville, NJ, USA). Illumina libraries were prepared using a modified KAPA protocol with the KAPA LTP Library Preparation Kit (Roche, Basel, Switzerland) with adaptor ligation and adaptor fill-in reactions based on Meyer and Kircher (2010). Some libraries have been instead prepared with the NEBNext Ultra II DNA PCR-free Library Prep Kit (New England Biolabs, Ipswich, MA, USA). Samples were either double indexed with a set of 60 dual-index primers, as recommended by Kircher et al. (2012) and described in Loiseau et al. (2019), or with Illumina TrueSeq PCR-free dual indexes. Finally, the libraries underwent size selection steps using AMPure Beads (Agencourt). Libraries were then pooled and sequenced at Vienna BioCenter Core Facilities on Illumina HiSeqV4 PE125 or on NovaSeqS1 PE150. Protocol details for all accessions are listed in Supporting Table S3.

Data Processing

The raw sequence data was demultiplexed using deML v.1.1.3 (Renaud et al. 2015) and bamtools v.2.5.1 (Barnett et al. 2011) and converted from BAM to fastq format using

bedtools v.2.29.2 (Quinlan and Hall 2010). Reads were trimmed for adapter content and quality using trimgalore v.0.6.5 (Krueger 2019), a wrapper tool around fastqc and cutadapt, using --fastqc --retain unpaired. Sequence quality and adapter removal were confirmed with FastQC v.0.11.9 (Andrews 2010).

Quality- and adapter-trimmed reads were aligned to the *T. fasciculata* reference genome v.1.0 (GenBank Assembly accession GCA_029168755.1, Groot Crego et al., 2023) using bowtie2 v.2.3.5.1 (Langmead and Salzberg 2012) with the --very-sensitive-local option to increase accuracy. Low-quality mapped reads were removed, alignments were sorted by position using samtools v.1.15.1 (Li et al. 2009), and PCR duplicates were marked using MarkDuplicates from PicardTools v.2.25.2 (Picard Toolkit 2018). Relatedness between accessions was inferred with kinship coefficients in KING v.2.2.6 (Manichaikul et al. 2010), both for confirming technical replicates and to infer unexpected relatedness. Samples with an average coverage below 2x or a first degree relationship (consistent with full-sib or direct parent-offspring relationships; i.e., kinship > 0.177) were removed from subsequent analysis (Supporting Table S3).

Next, variants were called using a dedicated pipeline available at https://github.com/giyany/TillandsiaPhylo. In brief, we used GATK HaplotypeCaller v.4.1.9.0 followed by joint calling with GenotypeGVCFs (Poplin et al. 2018). The resulting variant call file (VCF) was filtered to exclude indels and any SNPs 3bp or closer from indels using bcftools v.1.15 (Li 2011) and GATK SelectVariants (DePristo et al. 2011). Regions annotated as transportable elements were excluded using bedtools intersect (Quinlan and Hall 2010). We used the transition/transversion ratio as a guideline to define the filtering parameter values leading to a set of SNPs exhibiting the highest ratio, calculated with SnpSift

(Cingolani et al. 2012). The following filtering parameters were finally used: MQ < 15, DP < 4, QD < 4, FS > 40, SOR > 3, MAF < 0.045 and missing rate > 0.2. Summary statistics were generated using bcftools stats (Li 2011).

Phylogenetic Tree Inference

We inferred phylogenetic relationships for all samples using both a maximum-likelihood and a coalescent-based method. We included a coalescent-based method in order to explicitly account for gene tree incongruence, which may result in high support for an incorrect topology (Kubatko and Degnan 2007). Gene tree incongruence further provides insight into molecular genome evolution, including the extent of incomplete lineage sorting and other genomic processes such as hybridization and introgression (Galtier and Daubin 2008; Wendel and Doyle 1998). First, a concatenated matrix was prepared by converting a gVCF into a phylip file with vcf2phylip (Ortiz 2019). A maximum-likelihood tree was inferred on a dataset of concatenated SNPs with IQ-TREE v.1.6.12, using IQ-TREE's ModelFinder to select the best-fitting model and including an ascertainment bias correction (Nguyen et al. 2015, Kalyaanamoorthy et al., 2017). The available *T. zoquensis* accession grouped within *T. fasciculata* (Supporting Fig. S2), suggesting a need to revise its species status. After removing this sample, we constructed ML trees on a whole-genome, as well as on a chromosome-by-chromosome basis, on a concatenated supermatrix partitioned by genes including both variant and invariant sites. The matrix was prepared as described above and IQ-TREE 2's ModelFinder was used to select the best-fitting partitioning scheme and models. Node support was inferred with 1,000 nonparametric bootstrap replicates (Chernomor et al. 2016). To construct a species tree, ML trees were estimated on non-

overlapping genomic windows of 100kb after excluding windows with fewer than 40 SNPs. Since loci with insufficient signal may reduce the accuracy of species tree estimation (Mirarab 2019), nodes with a bootstrap support below ten were collapsed across all trees with Newick utilities v.1.1.0 (Junier and Zdobnov 2010). ASTRAL-III v.5.7.8 (hereafter: ASTRAL) was then used to infer a species tree, measuring branch support as posterior probabilities (Zhang et al. 2018). To explore gene tree discordance, we used phyparts to calculate quartet support for the main, alternative and second alternative topologies as well as the number of concordant and discordant bipartitions on each node with a cutoff of ten for informative bootstrap values (-s 10; Smith et al. 2015). Gene tree discordance was visualised with phypartspiecharts.py (available from https://github.com/mossmatters/MJPythonNotebooks).

Investigating Monophyly and Deviations from a Bifurcating Tree Structure

We used several variations of the ABBA-BABA test (D-statistic) to further explore the relationships within and between clades and to assess deviations from tree structure (Durand et al. 2011; Green et al. 2010; Martin et al. 2015). The D-statistic we implemented in Dsuite v.0.5r45 (Malinsky et al. 2021) specifically uses allele frequency estimates, which allows to include several individuals per taxon and does not require the implicit assumption that the outgroup is fixed for the ancestral allele (Malinsky et al. 2021). *Tillandsia complanata* was used as the outgroup for all comparisons. We first examined the consistency of assigning individuals to a clade. Following Malinsky et al. (2018), we tested whether individuals assigned to the same clade always share more derived alleles with each other than with individuals from another clade. For this comparison and all related D-statistics hereafter,

significance was assessed using a jackknife procedure with 200kb window size, and family-wise error rate (FWER) was calculated and corrected for multiple comparisons following the Holm–Bonferroni method with the p.adjust function in R (R Core Team 2020).

To further characterise the relationships among clades, we examined the consistency of clade monophyly within our set of window-based trees using the check_monophyly function in the ETE Toolkit v.3 (Huerta-Cepas et al. 2016). A cloudogram of ML trees was visualised using ggdensitree from the R package ggtree v.3.4.0 (Yu 2020). Trees were modified using R packages phytool v.1.0-3 (Revell 2012) and treeio v.1.20.0 (Wang et al. 2020), with branch lengths forced into ultrametric structure for visualisation purposes only. We next used D_{min}, another variation of the D-statistic (Malinsky et al. 2018), to assess if allele-sharing among clades is consistent with a tree-like structure. D_{min} measures the minimal amount of gene flow within a trio by providing the minimal absolute value of D across all possible arrangements within it. A significantly positive score signifies allele sharing that is inconsistent with a single species tree, even in the presence of incomplete lineage sorting. In addition, a principal components analysis (PCA) was performed with SNPRelate v.1.20.1 (Zheng et al. 2012) on a set of biallelic SNPs, filtered to allow a maximum of 10% missing data and pruned to be 10kb or more apart.

Finally, to quantify and visualise the relationship among clades along the genome we used topology weighting by iterative sampling of subtrees with *Twisst* v.0.2 (Martin and Van Belleghem 2017). This method considers all the possible topologies relating several taxonomic groups and quantifies the contribution of each individual taxon topology to the full tree, enabling to locate genomic regions that are associated with certain topologies. We focused on the three largest clades and reduced the number of possible topologies by

including only clades *T. extensa*, *T. utriculata* and *T. fasciculata*, then chose windows of 50 SNPs following the strategy of Martin and Van Belleghem (2017). Subtrees were produced by partitioning the VCF with the biostar497922 script from Jvarkit (Lindenbaum 2015) and ML trees were inferred for each window as described above. A summary of all topologies and visualisation of topologies along genomic coordinates were produced using the plot_twisst.R script, modified to avoid averaging the signal over regions with high rates of missing data (Martin and Van Belleghem 2017).

Characterising Hybridization and Introgression

To quantify the rates of hybridization between all species in our dataset, we obtained a genome-wide signal of introgression using the original implementation of the D-statistic and estimates of admixture fraction f (henceforth: f_4-ratio) in Dsuite v.0.5r45 (Malinsky et al. 2021). We additionally computed D-statistic for each reference chromosome, obtaining p-values using a jackknife procedure with windows of 150 SNPs. Given a certain level of uncertainty regarding the true relationship between species, we set no *a priori* knowledge of taxon relationships. Instead, Dsuite ordered each trio so that the BBAA pattern is more common, principally to focus on topologies with minimal discordant patterns.

Since groups that are involved in hybridization may share branches on a phylogenetic tree, a single hybridization event can present multiple correlated instances of significantly elevated D-statistic. This is especially expected when introgression involves ancestral lineages, hence affecting internal branches of a phylogenetic tree. We used Dsuite to calculate the *f*-branch metric (henceforth: f_b(C)), an estimator developed to create a summary of gene flow events with minimized correlation by utilising multiple $f4$-ratio calculations

(Malinsky et al. 2021). The f_b(C) results invited several hypotheses regarding hybridization events, which we examined by inferring a species network under a maximum pseudo-likelihood approach using PhyloNet v.3.8.0 (Cao et al. 2019; Than et al. 2008; Y. Yu and Nakhleh 2015), allowing different numbers of reticulation events. We reduced our sampling to one outgroup and 18 ingroup taxa to include representatives from each highly-supported clade and inferred ML trees on non-overlapping windows as previously described.

To investigate the signature of introgression on specific loci and to locate highly admixed loci in regions of interest (see Results), we used the Dinvestigate function implemented in Dsuite which calculates statistics suitable for analysis in sliding genomic windows. Our analysis was performed on windows of 50 SNPs with a step size of ten. The D-statistic itself shows large variance when applied to genomic windows (Martin et al. 2015), hence we used f_{dM}, a statistic designed to investigate introgression in small genomic windows. f_{dM} accounts for allele sharing across all possible taxon arrangements in a species trio (Malinsky et al. 2015; Martin et al. 2015). After finding a significantly elevated D-statistic on chromosome 18 involving *T. achyrostachys* (from *T. punctulata* clade) and most species in the CAM clade *T. fasciculata* (see Results), we investigated patterns of hybridization between *T. punctulata*, *T. butzii* and *T. achyrostachys* (P1, P2 and P3). This allowed us to account for phylogenomic relatedness (between *T. achyrostachys* and *T. punctulata*) and for similar photosynthetic syndromes (between *T. achyrostachys* and *T. butzii*). Species in the *T. punctulata* clade putatively possess an intermediate C3-CAM photosynthetic syndrom, as they tend to express intermediary values of stable carbon isotope ratios ($\delta^{13}C$: see Supporting Table S2, but see also Messerschmid et al. 2021) and exhibit small to intermediate tank structures. *T. achyrostachys* was documented to express the strongest CAM phenotype and

290 $\delta^{13}C$ values (−14.7; Crayn et al. 2015) within our sampling. We finally identified regions
291 exhibiting D-statistic values exceeding the 95% quantile of the distribution to gain insight
292 into the possible functional basis of genes that were involved in ancient hybridization.

293 **Results**

294 **Read Mapping and Variant Calling**

295 After removing samples with low coverage, those sharing high kinship coefficients, and the
296 *T. zoquensis* accession that clustered in an unexpected position we retained 64 *Tillandsia*
297 accessions, corresponding to 36 recognized species. The average number of reads retained
298 per accession was $5.11x10^7$ (range $4.7x10^6$-$1.2x10^8$, SD=$2.5x10^7$) and average mapping rates
299 were 89.6% (range 69.4%-97.5%, SD=6.31), with slightly higher rates for members of the *T.*
300 *fasciculata* clade and slightly lower for the SA clades (97.5% and 89.6% on average
301 respectively). The differences between the main clades (see below and Fig. 1) were not
302 significant (Kruskal–Wallis test, p-value = 0.22), suggesting no or limited biases towards the
303 used reference genome. An average sequence coverage of 11.5x (range 2.6x-26.6x, SD=5.0x)
304 was obtained. After variant calling and filtering (see Methods) we retained 2,162,143 high-
305 quality SNPs.

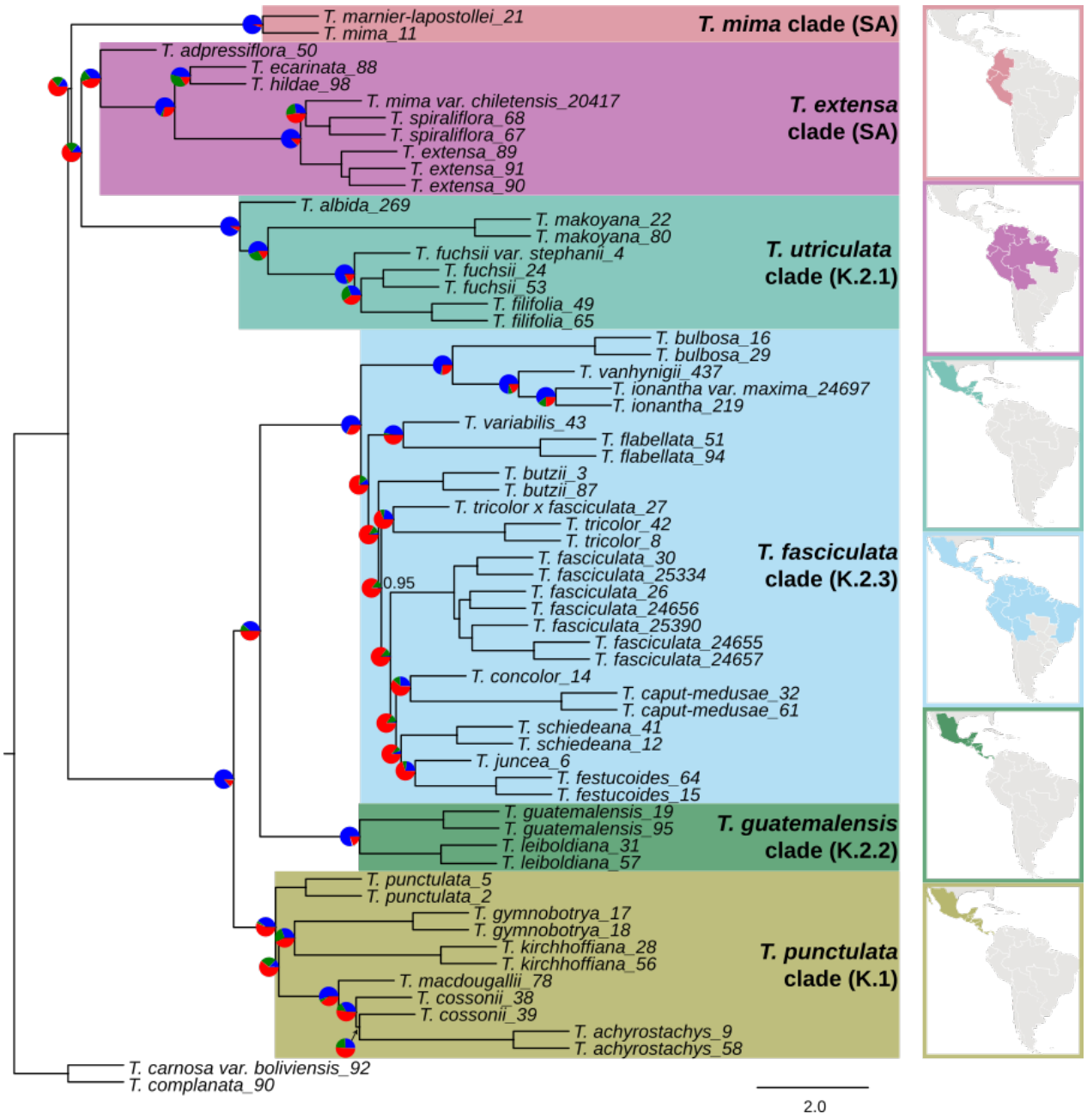

306 **Figure 1.** Coalescent-based species trees generated on 3,785 genomic windows with
307 ASTRAL-III for 64 individuals representing 34 species of *Tillandsia* subg. *Tillandsia*, plus

two outgroups. Branch lengths are given in coalescent units. Node values represent local posterior probabilities for the main topology and are equal to one unless noted otherwise. Pie charts at the nodes show levels of gene tree discordance: the percentages of concordant gene trees (blue), the top alternative bipartition (green), other conflicting topologies (red) and uninformative gene trees (grey).

Phylogenomic Inference Contradicts clade Monophyly

The concatenated matrix was partitioned to 14,392 genes and coalescent-based analyses were performed on 3,785 genomic windows. The species tree (Fig. 1) and concatenated maximum-likelihood (ML) tree (Supporting Fig. S1) yielded consistent results regarding the main clades and relationships. Contrary to among-clade relationships previously reported for this subgenus (Barfuss et al. 2016; Granados Mendoza et al. 2017; Rivera 2019; Vera-Paz et al., 2023), neither the South American species nor the Central American 'K' clades formed monophyletic groups. Instead, the South American species were separated into two clades: one consisted of endemic Peruvian species and the widespread species *T. adpressiflora*, placed as sister group to the T. *utriculata* clade (previously K.2.1), while a second clade contained *T. marnier-lapostollei* and *T. mima*. The clades do not correspond to the previously-inferred *T. paniculata* and *T. secunda* clades (Vera-Paz et al. 2003), hence we newly refer to them as *T. extensa* and *T. mima* clades, respectively.

'Clade K' was similarly recovered as polyphyletic. The *T. utriculata* clade (K.2.1), previously considered a sister to the clades of *T. fasciculata* (K.2.3) and of *T. guatemalensis* (K.2.2), was unexpectedly recovered as a sister to the South American *T. extensa* clade (thus

329 incongruent with a monophyly of the previous inferred 'clade K.2'). The assignment of
330 species to clades and all other relationships between sub-clades remained overall congruent
331 with previous phylogenies (Granados Mendoza et al. 2017; Vera-Paz et al., 2023). Several
332 within-clade topological differences appeared in trees inferred with different methods,
333 especially within the *T. fasciculata* clade. The latter were highly supported in the
334 concatenated tree yet coupled with high levels of gene tree incongruence (see below),
335 suggesting substantial allele sharing and high rates of gene flow within this clade.

336 Gene tree discordance was widespread within the dataset, affecting both deep and
337 shallow nodes (Fig. 1; Supporting Fig. S3). The relationships between the South American
338 species and the *T. utriculata* clade were characterised by short internode distances and many
339 alternative topologies. Frequently, the majority of inferred gene tree topologies were
340 discordant with a single main topology: for example, in the node preceding the separation of
341 the SA clades only 587 (15.5%) of all gene windows supported the main topology (Fig. 1;
342 Supporting Fig. S3). Similar levels of discordance characterised many of the internal nodes
343 within the *T. fasciculata* clade and high levels of discordance were also found within the
344 intermediate CAM clade *T. punctulata* (Fig. 1; Supporting Fig. S3).

345 Maximum-likelihood trees constructed separately for concatenated matrices of each
346 reference chromosome retrieved many different topologies: solely considering relationships
347 between main clades we recognized ten different topologies among the 25 different trees (see
348 Supporting file 1). The placement of the *T. mima* clade showed the greatest incongruence
349 between trees, as well as the placement of *T. adpressiflora*. Within-clade relationships, like
350 the whole-genome topology, were recovered from three chromosome-by-chromosome trees.
351 The South American species formed a monophyly in six chromosome trees and 'clade K' was

recovered as monophyletic in two. While each chromosome tree contains high amounts of gene tree discordance, the abundance of different topologies imply that several evolutionary histories can be traced along the genome of *Tillandsia*, as disparate genomic processes muddy the relationship between gene trees and the true species tree.

Lack of Monophyly and Deviations from Tree-like Structure

The multitude of tree topologies along the genome led us to hypothesise that a single bifurcating tree misrepresents the true relationships between Central American *Tillandsia* (i.e., previous 'clade K'). To investigate potential deviations from a tree-like structure, we analysed the patterns of allele sharing between species and between clades. Assuming no inter-specific gene-flow, allele sharing is expected to be consistent with the main tree topology, whereas asymmetrical allele sharing indicates deviations from that assumption.

We first calculated allele sharing between all species to test the robustness of the assignment of species to clades, utilising allele frequency estimates as performed with D-statistic. We found high support for clade monophyly, as species assigned to the same clade always shared more alleles with other species within the clade than with species from other clades. Except for the *T. punctulata* clade, consistency of clade monophyly was further supported in analyses performed in genomic windows: monophyly was confirmed in 92.0%, 79.4%, 67.0% and 39.7% of the windows for clades *T. utriculata*, *T. guatemalensis*, *T. fasciculata* and *T. punctulata*, respectively.

We next characterised allele sharing between clades by computing the D_{min} statistic for a total of 7,141 trios. We found widespread deviations from a tree-like structure, driven mostly by allele sharing between Central American taxa (previous 'clade K'): D_{min} values

were significantly elevated in 3,650 comparisons (P<0.05) with more than 95% of those being highly significant (P<0.01). The rate of significant D values was highest for comparisons involving accessions assigned to *T. utriculata* clade (58.7% of the trios), followed by *T. punctulata*, *T. guatemalensis* and *T. fasciculata* (57.9%, 56.1% and 51.4%, respectively; Supporting Fig. S4b). After distance-pruning and allowing for maximum 10% missing data we retained 16,204 SNPs for a PCA analysis. The analysis provided evidence for consistent interspecific genetic structure, separating the South American clades and the *T. utriculata* clade, while the remainder of the Central American clades clustered densely (Supporting Fig. S4c).

Finally, to obtain a better understanding of how clade relationships vary along the genome, we considered three distinct tree topologies for topology weighting with *Twisst*: the most frequent topology was congruent with the one recovered in the species tree, which placed the *T. extensa* clade as sister to the *T. utriculata clade* in 42% of the windows. A second topology, with the *T. fasciculata* and *T. utriculata* clades as sister clades, was recovered from 35% of the genomic windows while a third topology appeared in 23% (Supporting Fig. S5). The three topologies were broadly equally distributed along the genome – however, in some chromosomes 4 (for example, chromosome 4; Supporting Fig. S5) the first topology frequented the centromeric regions (discussed in Gill et al. 2008; Yan and Jiang 2007). Topology weighing is a descriptive method which does not explicitly test for introgression or ILS, hence, we could not discern the processes underlying the recovered phylogenetic signal. Regardless, the prevalence of the main topology in regions of low recombination rates and reduced genic density suggests that it represents the backbone phylogeny, while other topologies are likely the result of gene flow or deep coalescence.

Correlated and Widespread Gene-flow Events

D-statistics results for trios arranged to maximise the observed number of BBAA patterns indicated that all species in our dataset were involved in potential hybridization (Fig. 2). Out of 7,141 tests in total, 4,331 returned significantly elevated values, with D values ranging between 0.021 and 0.581. Chromosome-by-chromosome analyses found that the signal was not localised to a specific chromosome (Supporting file 2). A prominent signal revealed introgression between species in the *T. utriculata* clade and all other Central American clades. Notable gene-flow signals were also indicated within the *T. fasciculata* clade. *f*4-ratio scores ranged between 0.0017 and 0.357, but in most hybridization events the proportion of the genome involved was estimated as smaller than 10% (Supporting Fig. S6). A few exceptions where larger parts of the genome were admixed were found within the main clades: for example, *T. caput-medusae* was involved in two hybridization events with *T. butzii* and T. *fasciculata* involving ca 31.7% of the genome (Supporting Fig. S4).

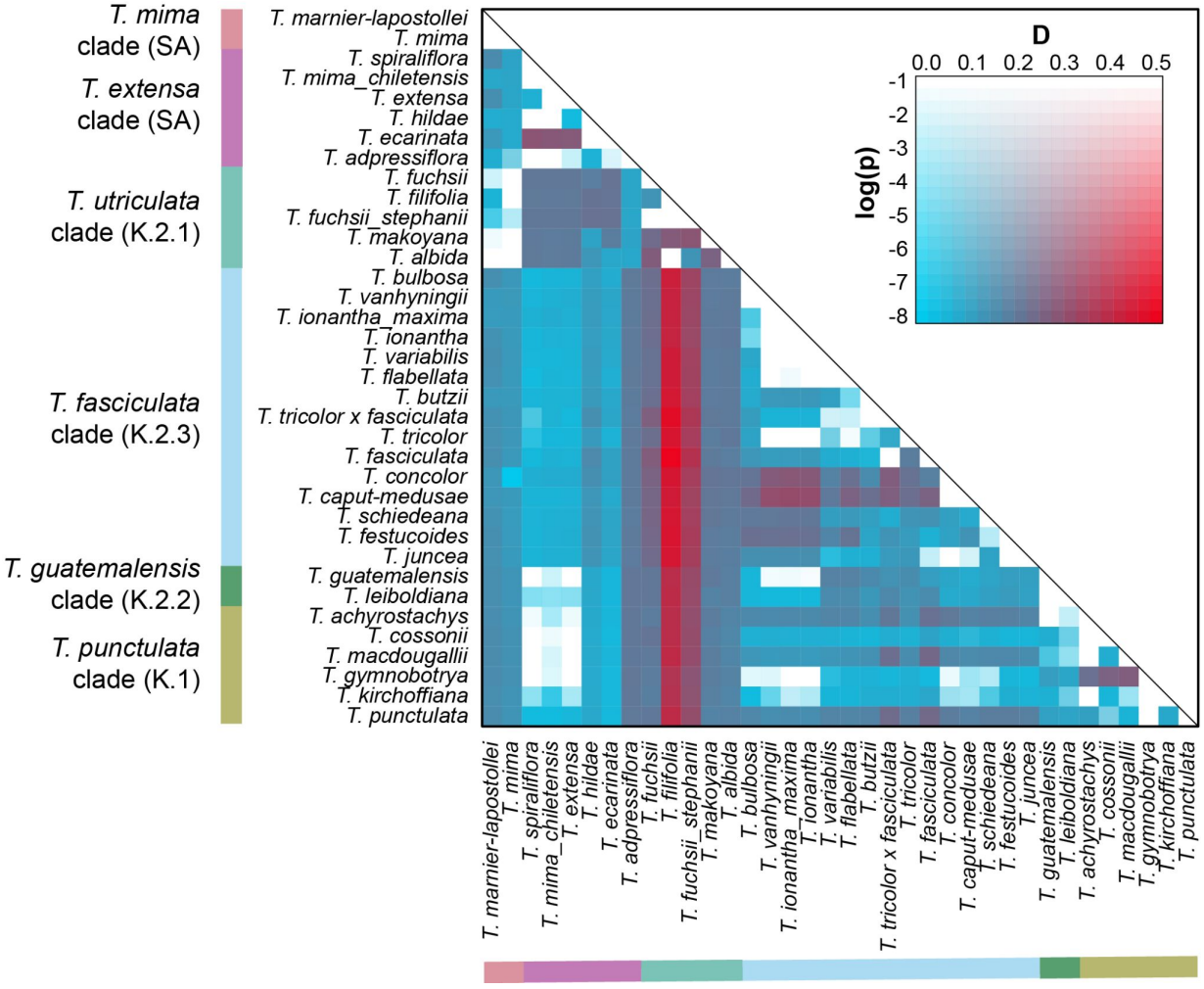

Figure 2. Heatmap summarizing 7,141 four-taxon D-statistic tests. *Tillandsia complanata* was used as the outgroup in all tests. The four taxa in each test have been rearranged to always obtain positive D values and P2 and P3 are shown on the axes. Colour indicates the value of D and the log value of p-value, the latter estimated using a block jackknife procedure with a 200kb window size and corrected for family-wise error rate. Colours on the bars correspond to the clades in Figure 1.

Further analysis suggested that past hybridization events involved the ancestor of the *T. urticulata* clade and an ancestor of the other three Central American clades. The f-branch metric assigned elevated $f_b(C)$ scores with an average of 5.9% to events involving these clades (Fig. 3). Networks were inferred in PhyloNet on a total of 3,337 windows. Analyses allowing for four reticulation events resulted in less than four events reported, so we present here results for up to three reticulations allowed (Fig. 4). The results repeatedly indicated the involvement of the *T. utriculata* clade in hybridization with both the South American *T. extensa* and the Central American clades, with notably higher weights assigned to the former. Additional gene-flow events occurred within clades: 16.9% of $f_b(C)$ values were significantly elevated ($P<0.05$), but most high values occurred for events within clades (Fig. 3). In addition, the f-branch values supported the identification of a cryptic hybrid sample (*T. tricolor* x *fasciculata*) as a hybrid between *T. tricolor* and *T. fasciculata*. Overall, these findings confirm the extensive violations of a tree-like structure revealed in the previous part of the analysis and suggest a frequent occurrence of inter-specific gene-flow throughout the evolutionary history of the radiation.

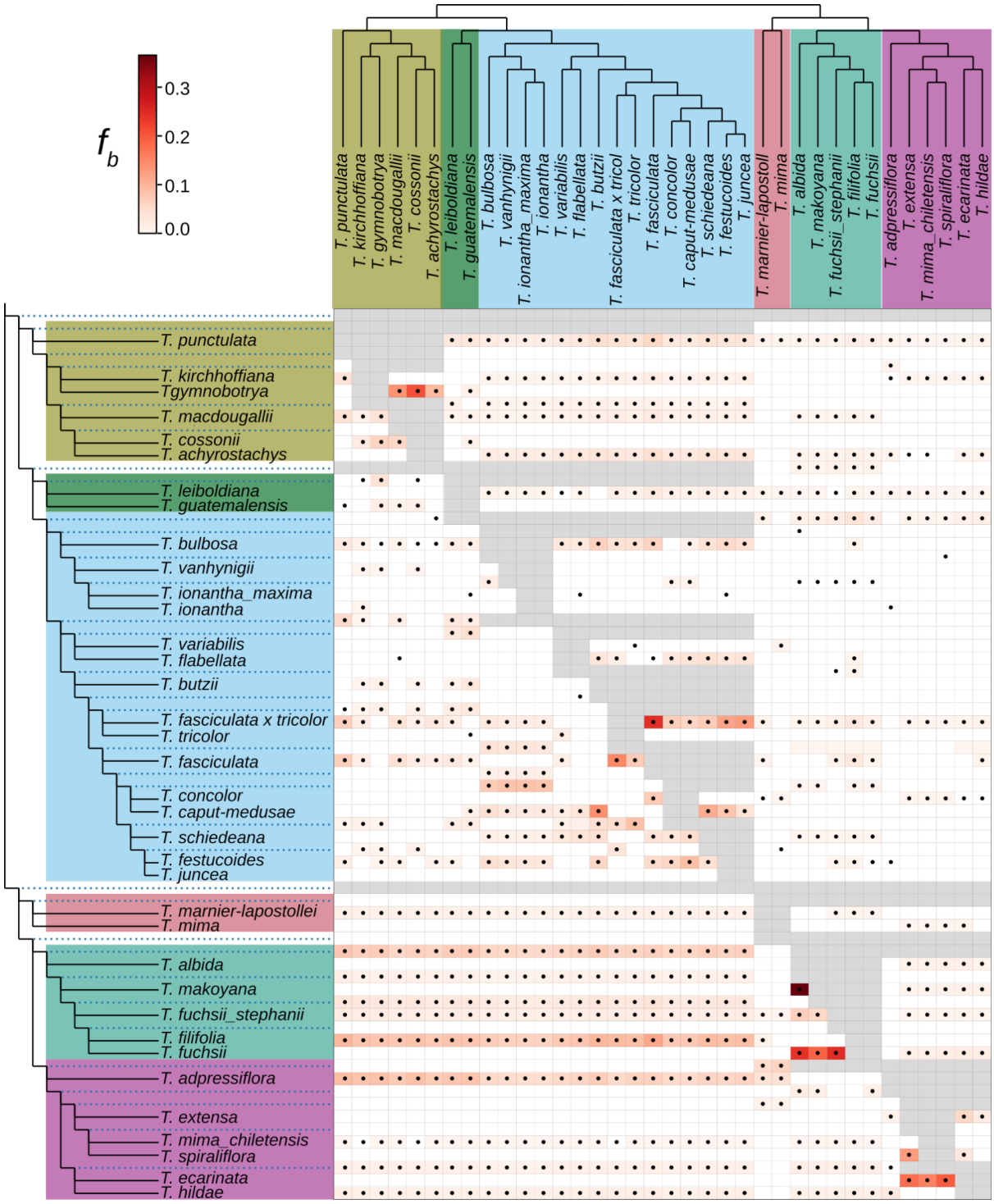

Figure 3. Heatmap summarising the statistic $f_b(C)$, where excess sharing of derived alleles is inferred between the branch of the tree on the Y axis and the species C on the X axis. The ASTRAL species tree was used as input topology for the branch statistic. The matrix is colored according to the legend of the $f_b(C)$ values and grey squares correspond to tests that are inconsistent with the ASTRAL phylogeny. Dots within the matrix denote a significant p-value, estimated using a block jackknife procedure and corrected for family wise error rate. Colours correspond to the clades in Figure 1.

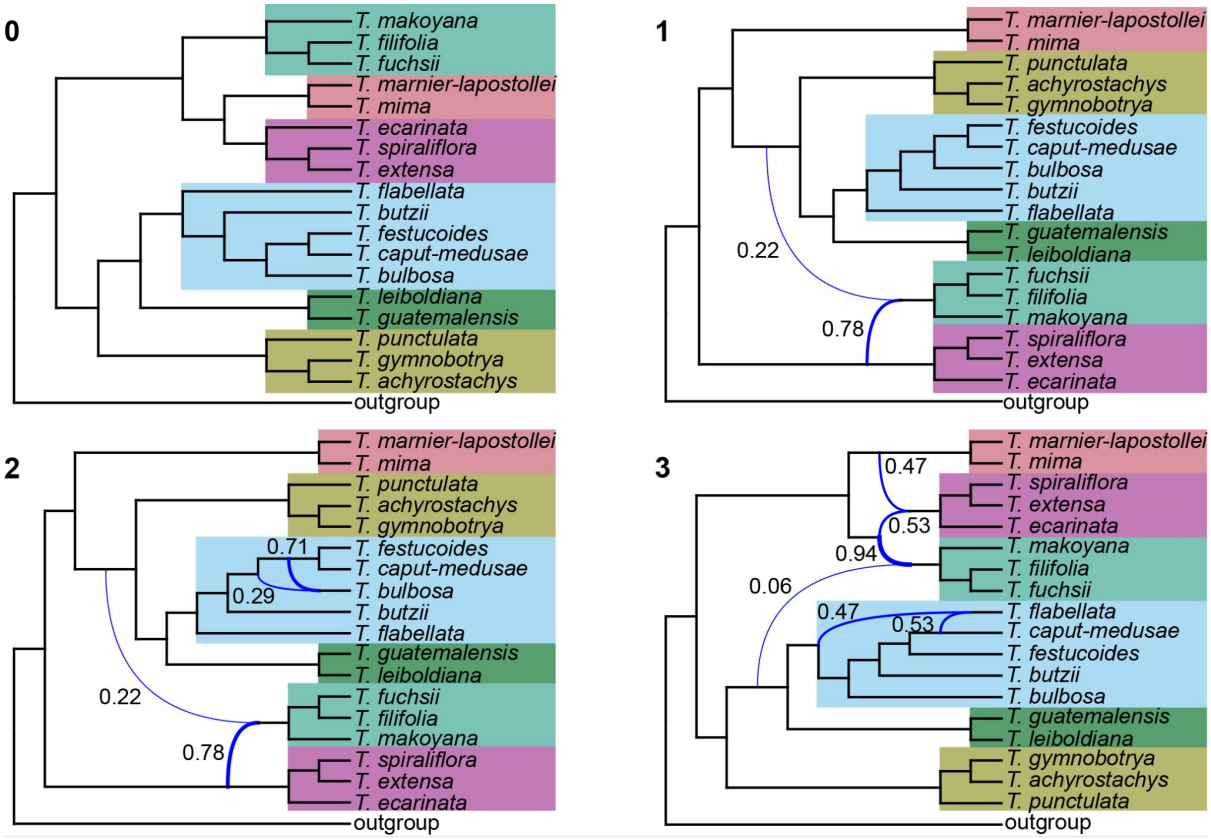

Figure 4. Best maximum pseudo-likelihood species networks inferred with PhyloNet for zero to three reticulation events. Curved branches indicate reticulation events. Numbers next to curved branches indicate inheritance probabilities for each event. Colours correspond to the clades in Figure 1.

Local footprint of introgression associated with photosynthetic syndrome

Elevated D-statistics, signifying introgression, generally affected all chromosomes (Supporting file 2). In contrast, a significantly elevated, but localized D-statistic was found on chromosome 18 involving *T. achyrostachys* (*T. punctulata* clade) and most of the species in the CAM clade *T. fasciculata* (Supporting file 2). To further investigate this elevated but highly localised signal, f_{dM} statistics were calculated on a total of 9,185 windows between *T. punctulata*, *T. butzii* and *T. achyrostachys*. The first and last species are assigned to the *T punctulata* clade whereas *T. butzii* is a member of the *T. fasciculata* clade. Across all chromosomes, mean values were negative at an average of -0.043 fitting the expectation for higher rates of gene flow between closely related species (Supporting Fig. S7). Chromosome 18 was however characterised by two regions of high positive values, which were also evident with topology weighting. Considering centromere localization, we found that the loci exhibiting high D-statistic values coincide with low genic density and contain 194 genes (Supporting Fig. S7). In a detailed survey of gene annotations, we found this set of genes were potentially associated with a variety of functions. For example, serine/threonine-protein kinase prpf4B is known to have a role in pre-mRNA splicing in yeast and humans (Eckert et al. 2016), and was found to be associated with stress response in millet (Parvathi et al. 2019).

Another example is the S-adenosyl-L-methionine-dependent methyltransferase superfamily protein (SAM-Mtase), a key enzyme in plant metabolic pathways like the phenylpropanoid and flavonoid pathway (Joshi and Chiang, 1998; Sistla and Rao 2004; Supporting Fig. S7).

Discussion

Hybridization is widely researched for its different roles in plant speciation. Based on a multi-species genomic dataset and phylogenomic approaches we highlight here the genus *Tillandsia* as a striking example of a highly reticulated radiation. The radiation likely proceeded in the presence of rampant inter-specific gene-flow, rather than by refined reproductive barriers (Loiseau et al. 2019; Koch et al. 2022; Vera-Paz 2023). An abundance of sequencing data tends to generate high branch support in both concatenated alignments and a coalescent-based tree-building method (Pease et al. 2016; Salichos and Rokas 2013), yet a detailed investigation in *Tillandsia* subg. *Tillandsia* revealed that a bifurcating tree offers an incomplete picture of the true relationships between species. Viewing reticulation as the genomic signature of cardinal molecular processes rather than uninformative ‘noise’, we offer a nuanced view into the complex evolutionary history of this Neotropic radiation. With that, *Tillandsia* provides a compelling example to the mounting evidence of the important contribution of gene flow in species diversification (Arnold et al. 2016; Filiault et al. 2018; Keller et al. 2013; Nosil 2008; Seehausen et al. 2014; Slovak et al. 2023; Stankowski et al. 2019; D. Zhang et al. 2021).

In stark contrast to previously inferred phylogenies, we retrieved the Central American ‘clade K’ as polyphyletic. First inferred based on morphological characters and

later on a limited number of genomic markers, the generic and sub-generic classification of subfamily Tillandsioideae in general and of the genus *Tillandsia* in particular shifted throughout decades of phylogenetic research. Overall, phylogenies based on plastid sequences and on relatively few nuclear genomic regions offered little resolution for shallow phylogenetic in this young genus, particularly within Central American taxa (Pinzón et al. 2016; Barfuss et al. 2016; Granados Mendoza et al. 2017). Recently, a full plastome phylogeny greatly improved the phylogenomic resolution while statistical support remained low in shallow nodes (Vera-Paz et al., 2023). We suggest that incongruence between *Tillandsia* phylogenies reflects both the local scarcity of genomic divergence within this young radiation and the complicating role of hybridization. Moreover, considering the prevalence of recent inter-specific gene-flow, the monophyly of the Central American clades within plastid phylogenies seems particularly driven by chloroplast capture (Pham et al., 2017). Beyond insight on clade relationship, our analyses produced several novel insights regarding cryptic species: for example, our inference suggests that *T. mima* and *T. mima var. chiletensis* are distinct species, despite morphological similarities. Similarly, *T. fuchsii* and *T. fuchsii* var. *stephanii* did not form a monophyletic clade, raising a need to revise their taxonomic status (Fig. 1; Supporting Fig. S1).

Hybridization played a central role in the evolution of Central American *Tillandsia*, reflected in departures from tree structure encompassing all clades and species. D-statistics revealed both recent and ancient gene flow while allele sharing did not compromise species or clade boundaries. Notably, the obtained $f_b(C)$ ranges were in general far higher than those previously inferred for ancestral introgressions between species of Malawi cichlids (Malinsky et al. 2018) or of hares (Ferreira et al. 2021), but comparable to other rapid radiations (De-

Kayne et al. 2022; Slovak et al. 2023; Suvorov et al. 2022). The interplay of genomic signals and our limited clade sampling complicate inference on the timing of gene-flow events, yet their high prevalence suggests they occured during both ancestral and recent history. High rates of gene flow are compatible with *Tillandsia* ecology and evolution: *Tillandsia* is known to produce natural hybrids (Luther 1985; Koch et al. 2022; Till 2000) and bears copious seed adapted to wind dispersal, which may facilitate high rates of inter- and intra-specific gene flow (Mondragon and Calvo-Irabien 2006; Victoriano-Romero et al., 2017). Previous studies proposed that the South American ancestor of *Tillandsia* subg. *Tillandsia* colonised North and Central America in a long-distance dispersal event 4.86 Mya (Barfuss et al. 2016; Granados Mendoza et al. 2017; Vera-Paz et al. 2023) and our results offer intriguing hypotheses on multiple, likely polytopic origins of Central American *Tillandsia*. Instead of a single dispersal event, South American ancestors may have dispersed in several migration events into Central America. Strong population bottlenecks, producing phylogenies with relatively long internal branches, were followed by concomitant episodes of gene admixture and increased isolation. It is further possible that gene-flow increased allelic diversity in founder populations, thus fueling adaptation (see below).

Apart from hybridization, other molecular processes can contribute to violations of a strictly bifurcating species tree, such as ILS, paralogy, and gene duplication and loss (Edwards 2009; Galtier and Daubin 2008; Smith et al. 2015). Previous studies on *Tillandsia* subg. *Tillandsia* indeed found evidence for changes in population sizes and elevated rates of gene duplication and loss, specifically associated with photosynthetic syndrome shifts (de La Harpe et al. 2020; Groot Crego et al. 2023; Yardeni et al. 2022). We suggest there is strong evidence for ancestral hybridization as the source of discordance between the *T. utriculata*

clade and other Central American clades: f-statistic and D-statistic tests are robust to the presence of ILS, as is PhyloNet (Malinsky et al. 2021; Martin et al. 2015; Wen et al. 2018) and ancestral population structure is unlikely to segregate through the demographic events that accompanied *Tillandsia*'s dispersal into Central America. Regardless, the generality of the obtained signal could be influenced by our limited sampling; a study employing a wider sampling could further infer if introgression involved related or ancient lineages, while considering disparate molecular processes.

Genetic variation introduced through hybridization can be maladaptive, neutral or adaptive (Moran et al., 2021; Wong et al 2022; Zeberg & Pääbo 2020). While its consequences remain difficult to predict and negative consequences may not be observable for long periods, an adaptive role of hybridization has been demonstrated in numerous animal and plant taxa (Arnold et al. 2016; Dasmahapatra et al. 2012; Lamichhaney et al. 2015; Leroy et al. 2020; Taylor and Larson 2019). In this study, we have identified two introgressed regions on chromosome 18, involving species that share a photosynthetic syndrome. Interestingly, the introgressed regions coincide with low gene density and one of them occurs at a chromosome edge. These findings echo the general expectation regarding the theory, posing that higher rates of introgression correlate with regions of low gene density, since introgressed fragments in gene-rich regions are more likely to be detrimental (Barton and Bengtsson, 1986; Martin and Jiggins 2017; Sankararaman et al. 2014). The incomplete taxon sampling in our current study limits our ability to draw generalities about adaptive introgression in *Tillandsia*: however, the conspicuously rapid accumulation of morphological and physiological disparity suggests that hybridization in *Tillandsia* may have contributed to its success in a wide range of habitats, potentially introducing novel alleles through porous

549 species boundaries and driving this evolutionary radiation. Further efforts will be needed to
550 identify additional potential adaptive regions and uncover the key genes within.

551 We used whole-genome sequencing to deeply investigate the phylogenomics of a
552 remarkable *Tillandsia* radiation. Recent research addressed questions on the genus'
553 evolutionary history, simultaneously expanding bromeliad and *Tillandsia* genomic resources
554 and facilitating a range of evolutionary analyses. Ultimately, the complex history of
555 *Tillandsia* retains elusiveness and invites further investigations to uncover the interplay of
556 processes that drove this rapid diversification. Future studies employing both a wider
557 sampling and a deeper genomic coverage can characterise the genomic properties associated
558 with diversification and explore the prevalence of hybridization across different evolutionary
559 scales.

560 **Acknowledgements**

561 This research was supported with funding from the Christian Lexer professorship start-up
562 BE772002 at the University of Vienna, and the FWF grant P35275 to O.P. The analyses took
563 advantage of the Vienna Scientific Cluster (VSC). We thank Magnus Nordborg, James Pease
564 and Hannes Svardal for insightful discussions and advice. We thank the members of Swiss
565 SNSF Sinergia project CRSII3_147630 and Juan P. Pinzón for accession sampling.

References

Abbott R., Albach D., Ansell S., Arntzen J.W., Baird S.J.E., Bierne N., Boughman J., Brelsford A., Buerkle C.A., Buggs R., Butlin R.K., Dieckmann U., Eroukhmanoff F., Grill A., Cahan S.H., Hermansen J.S., Hewitt G., Hudson A.G., Jiggins C., Jones J., Keller B., Marczewski T., Mallet J., Martinez-Rodriguez P., Möst M., Mullen S., Nichols R., Nolte A.W., Parisod C., Pfennig K., Rice A.M., Ritchie M.G., Seifert B., Smadja C.M., Stelkens R., Szymura J.M., Väinölä R., Wolf J.B.W., Zinner D. 2013. Hybridization and speciation. *J. Evol. Biol*. 26:229–246.

Andrews S. 2010. FastQC: a quality control tool for high throughput sequence data. Available online at: http://www.bioinformatics.babraham.ac.uk/projects/fastqc/

Arnold B.J., Lahner B., DaCosta J.M., Weisman C.M., Hollister J.D., Salt D.E., Bomblies K., Yant L. 2016. Borrowed alleles and convergence in serpentine adaptation. *Proc. Natl. Acad. Sci*. 113:8320–8325.

Barfuss M.H.J., Samuel R., Till W., Stuessy T.F. 2005. Phylogenetic relationships in subfamily Tillandsioideae (Bromeliaceae) based on DNA sequence data from seven plastid regions. *Am. J. Bot*. 92:337–351.

582 Barfuss M.H.J., Till W., Leme E.M.C., Pinzón J.P., Manzanares J.M., Halbritter H., Samuel
583 R., Brown G.K. 2016. Taxonomic revision of Bromeliaceae subfam. Tillandsioideae based on
584 a multi-locus DNA sequence phylogeny and morphology. *Phytotaxa*. 279:1–97.

585 Barnett D.W., Garrison E.K., Quinlan A.R., Strömberg M.P., Marth G.T. 2011. BamTools: a
586 C++ API and toolkit for analyzing and managing BAM files. *Bioinformatics*. 27:1691–1692.

587 Barth J.M.I., Gubili C., Matschiner M., Tørresen O.K., Watanabe S., Egger B., Han Y.-S.,
588 Feunteun E., Sommaruga R., Jehle R., Schabetsberger R. 2020. Stable species boundaries
589 despite ten million years of hybridization in tropical eels. *Nat. Commun*. 11:1433.

590 Barton N., Bengtsson B.O. 1986. The barrier to genetic exchange between hybridising
591 populations. *Heredity*. 57:357–376.

592 Benzing D.H. 2000. *Bromeliaceae: profile of an adaptive radiation*. Cambridge University
593 Press.

594 Boschman L.M., Condamine F.L. 2022. Mountain radiations are not only rapid and recent:
595 Ancient diversification of South American frog and lizard families related to Paleogene
596 Andean orogeny and Cenozoic climate variations. *Glob. Planet. Change*. 208:103704.

597 Cao Z., Zhu J., Nakhleh L. 2019. Empirical performance of tree-based inference of
598 phylogenetic networks. *19th Int. Workshop Algorithms Bioinformatics (WABI 2019)*. Schloss
599 Dagstuhl-Leibniz-Zentrum fuer Informatik.

600 Chernomor O., von Haeseler A., Minh B.Q. 2016. Terrace aware data structure for
601 phylogenomic inference from supermatrices. *Syst. Biol*. 65:997-1008.

602 Chew T., De Luna E., González D. 2010. Phylogenetic relationships of the pseudobulbous
603 *Tillandsia* species (Bromeliaceae) inferred from cladistic analyses of ITS 2, 5.8 S ribosomal
604 RNA gene, and ETS sequences. *Syst. Bot.* 35:86–95.

605 Cingolani P., Platts A., Wang L.L., Coon M., Nguyen T., Wang L., Land S.J., Lu X., Ruden
606 D.M. 2012. A program for annotating and predicting the effects of single nucleotide
607 polymorphisms, SnpEff. *Fly*. 6:80–92.

608 Cody S., Richardson J.E., Rull V., Ellis C., Pennington R.T. 2010. The Great American
609 Biotic Interchange revisited. *Ecography*. 33:326–332.

610 Crayn D.M., Winter K., Schulte K., Smith J.A.C. 2015. Photosynthetic pathways in
611 Bromeliaceae: phylogenetic and ecological significance of CAM and C3 based on carbon
612 isotope ratios for 1893 species. *Bot. J. Linn. Soc*. 178:169–221.

613 Dasmahapatra K.K., Walters J.R., Briscoe A.D., Davey J.W., Whibley A., Nadeau N.J.,
614 Zimin A.V., Hughes D.S.T., Ferguson L.C., Martin S.H., Salazar C., Lewis J.J., Adler S.,
615 Ahn S.-J., Baker D.A., Baxter S.W., Chamberlain N.L., Chauhan R., Counterman B.A.,
616 Dalmay T., Gilbert L.E., Gordon K., Heckel D.G., Hines H.M., Hoff K.J., Holland P.W.H.,
617 Jacquin-Joly E., Jiggins F.M., Jones R.T., Kapan D.D., Kersey P., Lamas G., Lawson D.,
618 Mapleson D., Maroja L.S., Martin A., Moxon S., Palmer W.J., Papa R., Papanicolaou A.,
619 Pauchet Y., Ray D.A., Rosser N., Salzberg S.L., Supple M.A., Surridge A., Tenger-Trolander
620 A., Vogel H., Wilkinson P.A., Wilson D., Yorke J.A., Yuan F., Balmuth A.L., Eland C.,
621 Gharbi K., Thomson M., Gibbs R.A., Han Y., Jayaseelan J.C., Kovar C., Mathew T., Muzny
622 D.M., Ongeri F., Pu L.-L., Qu J., Thornton R.L., Worley K.C., Wu Y.-Q., Linares M., Blaxter
623 M.L., ffrench-Constant R.H., Joron M., Kronforst M.R., Mullen S.P., Reed R.D., Scherer
624 S.E., Richards S., Mallet J., Owen McMillan W., Jiggins C.D., The Heliconius Genome
625 Consortium. 2012. Butterfly genome reveals promiscuous exchange of mimicry adaptations
626 among species. *Nature*. 487:94–98.

627 Davey J.W., Hohenlohe P.A., Etter P.D., Boone J.Q., Catchen J.M., Blaxter M.L. 2011.
628 Genome-wide genetic marker discovery and genotyping using next-generation sequencing.
629 *Nat. Rev. Genet*. 12:499–510.

630 Degnan J.H., DeGiorgio M., Bryant D., Rosenberg N.A. 2009. Properties of consensus
631 methods for inferring species trees from gene trees. *Syst. Biol.* 58:35–54.

De-Kayne R., Selz O.M., Marques D.A., Frei D., Seehausen O., Feulner P.G.D. 2022. Hybridization and a mixture of small and large-effect loci facilitate adaptive radiation. *bioRxiv*:2022.02.18.481029.

DePristo M.A., Banks E., Poplin R., Garimella K.V., Maguire J.R., Hartl C., Philippakis A.A., del Angel G., Rivas M.A., Hanna M., McKenna A., Fennell T.J., Kernytsky A.M., Sivachenko A.Y., Cibulskis K., Gabriel S.B., Altshuler D., Daly M.J. 2011. A framework for variation discovery and genotyping using next-generation DNA sequencing data. *Nat. Genet.* 43:491–498.

Doyle J.J., Doyle J.L., editors. 1987. A rapid DNA isolation procedure for small quantities of fresh leaf tissue. *Phytochem. Bull*. 19:11–15.

Drummond C.S., Eastwood R.J., Miotto S.T.S., Hughes C.E. 2012. Multiple continental radiations and correlates of diversification in Lupinus (Leguminosae): testing for key innovation with incomplete taxon sampling. *Syst. Biol*. 61:443–460.

Durand E.Y., Patterson N., Reich D., Slatkin M. 2011. Testing for ancient admixture between closely related populations. *Mol. Biol. Evol*. 28:2239–2252.

Eckert D., Andrée N., Razanau A., Zock-Emmenthal S., Lützelberger M., Plath S., Schmidt H., Guerra-Moreno A., Cozzuto L., Ayté J., Käufer N.F. 2016. Prp4 kinase grants the license

649 to splice: control of weak splice sites during spliceosome activation. *PLOS Genet*.
650 12:e1005768.

651 Edelman N.B., Frandsen P.B., Miyagi M., Clavijo B., Davey J., Dikow R.B., García-
652 Accinelli G., Van Belleghem S.M., Patterson N., Neafsey D.E., Challis R., Kumar S.,
653 Moreira G.R.P., Salazar C., Chouteau M., Counterman B.A., Papa R., Blaxter M., Reed R.D.,
654 Dasmahapatra K.K., Kronforst M., Joron M., Jiggins C.D., McMillan W.O., Di Palma F.,
655 Blumberg A.J., Wakeley J., Jaffe D., Mallet J. 2019. Genomic architecture and introgression
656 shape a butterfly radiation. *Science*. 366:594–599.

657 Edwards S.V. 2009. Is a new and general theory of molecular systematics merging?
658 *Evolution*. 63:1–19.

659 Espejo-Serna A., López-Ferrari A.R., Ramírez-Morillo I., Holst B.K., Luther H.E., Till W.
660 2004. Checklist of Mexican Bromeliaceae with notes on species distribution and levels of
661 endemism. *Selbyana*. 25:33–86.

662 Ferreira M.S., Jones M.R., Callahan C.M., Farelo L., Tolesa Z., Suchentrunk F., Boursot P.,
663 Mills L.S., Alves P.C., Good J.M., Melo-Ferreira J. 2021. The legacy of recurrent
664 introgression during the radiation of hares. *Syst. Biol*. 70:593–607.

665 Filiault D.L., Ballerini E.S., Mandáková T., Aköz G., Derieg N.J., Schmutz J., Jenkins J.,
666 Grimwood J., Shu S., Hayes R.D., Hellsten U., Barry K., Yan J., Mihaltcheva S., Karafiátová

667 M., Nizhynska V., Kramer E.M., Lysak M.A., Hodges S.A., Nordborg M. 2018. The
668 *Aquilegia* genome provides insight into adaptive radiation and reveals an extraordinarily
669 polymorphic chromosome with a unique history. *eLife*. 7:e36426.

670 Galtier N., Daubin V. 2008. Dealing with incongruence in phylogenomic analyses. *Philos.*
671 *Trans. R. Soc. B Biol. Sci*. 363:4023–4029.

672 Giarla T.C., Esselstyn J.A. 2015. The challenges of resolving a rapid, recent radiation:
673 empirical and simulated phylogenomics of Philippine shrews. *Syst. Biol*. 64:727–740.

674 Gill N., Hans C.S., Jackson S. 2008. An overview of plant chromosome structure. *Cytogenet.*
675 *Genome Res*. 120:194–201.

676 Givnish T.J. 2015. Adaptive radiation versus 'radiation' and 'explosive diversification': why
677 conceptual distinctions are fundamental to understanding evolution. *New Phytol*. 207:297–
678 303.

679 Givnish T.J., Barfuss M.H.J., Ee B.V., Riina R., Schulte K., Horres R., Gonsiska P.A.,
680 Jabaily R.S., Crayn D.M., Smith J.A.C., Winter K., Brown G.K., Evans T.M., Holst B.K.,
681 Luther H., Till W., Zizka G., Berry P.E., Sytsma K.J. 2011. Phylogeny, adaptive radiation,
682 and historical biogeography in Bromeliaceae: Insights from an eight-locus plastid phylogeny.
683 *Am. J. Bot*. 98:872–895.

684 Givnish T.J., Barfuss M.H.J., Ee B.V., Riina R., Schulte K., Horres R., Gonsiska P.A.,
685 Jabaily R.S., Crayn D.M., Smith J.A.C., Winter K., Brown G.K., Evans T.M., Holst B.K.,
686 Luther H., Till W., Zizka G., Berry P.E., Sytsma K.J. 2014. Adaptive radiation, correlated
687 and contingent evolution, and net species diversification in Bromeliaceae. *Mol. Phylogenet.*
688 *Evol*. 71:55–78.

689 Granados Mendoza C., Granados-Aguilar X., Donadío S., Salazar G.A., Flores-Cruz M.,
690 Hágsater E., Starr J.R., Ibarra-Manríquez G., Fragoso-Martínez I., Magallón S. 2017.
691 Geographic structure in two highly diverse lineages of *Tillandsia* (Bromeliaceae). *Botany*.
692 95:641–651.

693 Green R.E., Krause J., Briggs A.W., Maricic T., Stenzel U., Kircher M., Patterson N., Li H.,
694 Zhai W., Fritz M.H.-Y., Hansen N.F., Durand E.Y., Malaspinas A.-S., Jensen J.D., Marques-
695 Bonet T., Alkan C., Prüfer K., Meyer M., Burbano H.A., Good J.M., Schultz R., Aximu-Petri
696 A., Butthof A., Höber B., Höffner B., Siegemund M., Weihmann A., Nusbaum C., Lander
697 E.S., Russ C., Novod N., Affourtit J., Egholm M., Verna C., Rudan P., Brajkovic D., Kucan
698 Ž., Gušic I., Doronichev V.B., Golovanova L.V., Lalueza-Fox C., de la Rasilla M., Fortea J.,
699 Rosas A., Schmitz R.W., Johnson P.L.F., Eichler E.E., Falush D., Birney E., Mullikin J.C.,
700 Slatkin M., Nielsen R., Kelso J., Lachmann M., Reich D., Pääbo S. 2010. A draft sequence of
701 the Neandertal genome. *Science*. 328:710–722.

702 Groot Crego C., Hess J., Yardeni G., de La Harpe M., Priemer C., Beclin F., Saadain S.,
703 Cauz-Santos L.A., Temsch E.M., Weiss-Schneeweiss H., Barfuss M.H.J., Till W.,

704 Weckwerth W., Heyduk K., Lexer C., Paun O., Leroy, T. 2023. CAM evolution is associated
705 with gene family expansion in an explosive bromeliad radiation. *bioRxiv*, 2023-11. doi:
706 https://doi.org/10.1101/2023.02.01.526631

707 Harrison R.G., Larson E.L. 2014. Hybridization, introgression, and the nature of species
708 boundaries. *J. Hered*. 105:795–809.

709 Hibbins M.S., Gibson M.J., Hahn M.W. 2020. Determining the probability of hemiplasy in
710 the presence of incomplete lineage sorting and introgression. *eLife*. 9:e63753.

711 Hudlow W.R., Krieger R., Meusel M., Sehhat J.C., Timken M.D., Buoncristiani M.R. 2011.
712 The NucleoSpin® DNA Clean-up XS kit for the concentration and purification of genomic
713 DNA extracts: an alternative to microdialysis filtration. *Forensic Sci. Int. Genet*. 5:226–230.

714 Huerta-Cepas J., Serra F., Bork P. 2016. ETE 3: Reconstruction, Analysis, and Visualization
715 of Phylogenomic Data. *Mol. Biol. Evol*. 33:1635–1638.

716 Hughes C.E., Atchison G.W. 2015. The ubiquity of alpine plant radiations: from the Andes to
717 the Hengduan Mountains. *New Phytol*. 207:275–282.

718 Hughes C.E., Nyffeler R., Linder H.P. 2015. Evolutionary plant radiations: where, when, why
719 and how? *New Phytol*. 207:249–253.

720 Joshi C.P., Chiang V.L. 1998. Conserved sequence motifs in plant S-adenosyl-L-methionine-
721 dependent methyltransferases. *Plant Mol. Biol*. 37:663–674.

722 Junier T., Zdobnov E.M. 2010. The Newick utilities: high-throughput phylogenetic tree
723 processing in the UNIX shell. *Bioinforma. Oxf. Engl*. 26:1669–1670.

724 Kalyaanamoorthy S., Minh B.Q., Wong T.K., Von Haeseler A. and Jermiin L.S., 2017.
725 ModelFinder: fast model selection for accurate phylogenetic estimates. *Nature methods*,
726 14:587-589.

727 Keller I., Wagner C.E., Greuter L., Mwaiko S., Selz O.M., Sivasundar A., Wittwer S.,
728 Seehausen O. 2013. Population genomic signatures of divergent adaptation, gene flow and
729 hybrid speciation in the rapid radiation of Lake Victoria cichlid fishes. *Mol. Ecol*. 22:2848–
730 2863.

731 Kircher M., Sawyer S., Meyer M. 2012. Double indexing overcomes inaccuracies in
732 multiplex sequencing on the Illumina platform. *Nucleic Acids Res*. 40:e3.

733 Koch M. A., Kiefer C., Möbus J., Quandt D., Merklinger F., Harpke D., Benavides, F. V.
734 2022. Range expansion and contraction of *Tillandsia landbeckii* lomas in the hyperarid
735 Chilean Atacama Desert indicates ancient introgression and geneflow. *Perspect. Plant Ecol.*
736 *Evol. Syst*. 56:125689.

737 Krueger F. 2019. Trim Galore: a wrapper tool around Cutadapt and FastQC to consistently
738 apply quality and adapter trimming to FastQ files. *Babraham Bioinformatics, Babraham*
739 *Institute, Cambridge, United Kingdom*.

740 Kubatko, L. S., Degnan, J. H. 2007. Inconsistency of phylogenetic estimates from
741 concatenated data under coalescence. *Syst. Biol*. 56:17-24.

742 de La Harpe M., Paris M., Hess J., Barfuss M.H.J., Serrano-Serrano M.L., Ghatak A.,
743 Chaturvedi P., Weckwerth W., Till W., Salamin N., Wai C.M., Ming R., Lexer C. 2020.
744 Genomic footprints of repeated evolution of CAM photosynthesis in a Neotropical species
745 radiation. *Plant Cell Environ*. 43:2987-3001.

746 de La Harpe M., Paris M., Karger D.N., Rolland J., Kessler M., Salamin N., Lexer C. 2017.
747 Molecular ecology studies of species radiations: current research gaps, opportunities and
748 challenges. *Mol. Ecol*. 26:2608–2622.

749 Lagomarsino L.P., Condamine F.L., Antonelli A., Mulch A., Davis C.C. 2016. The abiotic
750 and biotic drivers of rapid diversification in Andean bellflowers (Campanulaceae). *New*
751 *Phytol*. 210:1430–1442.

752 Lamichhaney S., Berglund J., Almén M.S., Maqbool K., Grabherr M., Martinez-Barrio A.,
753 Promerová M., Rubin C.-J., Wang C., Zamani N., Grant B.R., Grant P.R., Webster M.T.,

754 Andersson L. 2015. Evolution of Darwin's finches and their beaks revealed by genome
755 sequencing. *Nature*. 518:371–375.

756 Langmead B., Salzberg S.L. 2012. Fast gapped-read alignment with Bowtie 2. *Nat. Methods*.
757 9:357–359.

758 Leroy T., Louvet J.-M., Lalanne C., Le Provost G., Labadie K., Aury J.-M., Delzon S.,
759 Plomion C., Kremer A. 2020. Adaptive introgression as a driver of local adaptation to climate
760 in European white oaks. *New Phytol*. 226:1171-1182.

761 Li H. 2011. A statistical framework for SNP calling, mutation discovery, association mapping
762 and population genetical parameter estimation from sequencing data. *Bioinformatics*.
763 27:2987–2993.

764 Li H., Handsaker B., Wysoker A., Fennell T., Ruan J., Homer N., Marth G., Abecasis G.,
765 Durbin R. 2009. The sequence alignment/map format and SAMtools. *Bioinformatics*.
766 25:2078–2079.

767 Linck E., Battey C.J. 2019. On the relative ease of speciation with periodic gene flow.
768 *bioRxiv*.:758664.

769 Lindenbaum P. 2015. JVarkit: java-based utilities for Bioinformatics. [Computer software].
770 https://doi.org/10.6084/m9.figshare.1425030

771 Linder H.P. 2008. Plant species radiations: where, when, why? *Philos. Trans. R. Soc*. B Biol.
772 Sci. 363:3097–3105.

773 Loiseau O., Olivares I., Paris M., de La Harpe M., Weigand A., Koubínová D., Rolland J.,
774 Bacon C.D., Balslev H., Borchsenius F., Cano A., Couvreur T.L.P., Delnatte C., Fardin F.,
775 Gayot M., Mejía F., Mota-Machado T., Perret M., Roncal J., Sanin M.J., Stauffer F., Lexer
776 C., Kessler M., Salamin N. 2019. Targeted capture of hundreds of nuclear genes unravels
777 phylogenetic relationships of the diverse Neotropical palm tribe Geonomateae. *Front. Plant*
778 *Sci*. 10:864.

779 Luther, H. E. 1985. Notes on hybrid tillandsias in Florida. *Phytologia.* 53:175–176.

780 Malinsky M., Challis R.J., Tyers A.M., Schiffels S., Terai Y., Ngatunga B.P., Miska E.A.,
781 Durbin R., Genner M.J., Turner G.F. 2015. Genomic islands of speciation separate cichlid
782 ecomorphs in an East African crater lake. Science. 350:1493–1498.
783 Malinsky M., Matschiner M., Svardal H. 2021. Dsuite - Fast D-statistics and related
784 admixture evidence from VCF files. *Mol. Ecol. Resour*. 21:584–595.

785 Malinsky M., Svardal H., Tyers A.M., Miska E.A., Genner M.J., Turner G.F., Durbin R.
786 2018. Whole-genome sequences of Malawi cichlids reveal multiple radiations interconnected
787 by gene flow. *Nat. Ecol. Evol*. 2:1940–1955.

788 Mallet J., Besansky N., Hahn M.W. 2016. How reticulated are species? *BioEssays*. 38:140–
789 149.

790 Manichaikul A., Mychaleckyj J.C., Rich S.S., Daly K., Sale M., Chen W.-M. 2010. Robust
791 relationship inference in genome-wide association studies. *Bioinformatics*. 26:2867–2873.

792 Martin S.H., Davey J.W., Jiggins C.D. 2015. Evaluating the use of ABBA–BABA statistics
793 to locate introgressed loci. Mol. Biol. Evol. 32:244–257.

794 Martin S.H., Jiggins C.D. 2017. Interpreting the genomic landscape of introgression. *Curr.*
795 *Opin. Genet. Dev*. 47:69–74.

796 Martin S.H., Van Belleghem S.M. 2017. Exploring evolutionary relationships across the
797 genome using topology weighting. *Genetics*. 206:429–438.

798 Meier J.I., Stelkens R.B., Joyce D.A., Mwaiko S., Phiri N., Schliewen U.K., Selz O.M.,
799 Wagner C.E., Katongo C., Seehausen O. 2019. The coincidence of ecological opportunity
800 with hybridization explains rapid adaptive radiation in Lake Mweru cichlid fishes. *Nat.*
801 *Commun*. 10:5391.

802 Messerschmid T.F.E., Wehling J., Bobon N., Kahmen A., Klak C., Los J.A., Nelson D.B.,
803 dos Santos P., de Vos J.M., Kadereit G. 2021. Carbon isotope composition of plant

804 photosynthetic tissues reflects a Crassulacean Acid Metabolism (CAM) continuum in the
805 majority of CAM lineages. *Perspect. Plant Ecol. Evol. Syst*. 51:125619.

806 Meyer M., Kircher M. 2010. Illumina sequencing library preparation for highly multiplexed
807 target capture and sequencing. *Cold Spring Harb. Protoc*. 2010:pdb.prot5448.

808 Mirarab S. 2019. Species tree estimation using ASTRAL: practical considerations.
809 *ArXiv*:1904.03826.

810 Mondragon D., Calvo-Irabien, L. M. 2006. Seed dispersal and germination of the epiphyte
811 Tillandsia brachycaulos (Bromeliaceae) in a tropical dry forest, Mexico. *Southwest. Nat.*
812 *51:462-470.*

813 Morales-Briones D.F., Kadereit G., Tefarikis D.T., Moore M.J., Smith S.A., Brockington
814 S.F., Timoneda A., Yim W.C., Cushman J.C., Yang Y. 2021. Disentangling sources of gene
815 tree discordance in phylogenomic data sets: testing ancient hybridizations in Amaranthaceae
816 s.l. *Syst. Biol*. 70:219–235.

817 Moran, B. M., Payne C., Langdon Q., Powell D. L., Brandvain Y., Schumer M. 2021. The
818 genomic consequences of hybridization. *Elife, 10*: e69016.

819 Naciri Y., Linder H.P. 2020. The genetics of evolutionary radiations. *Biol. Rev*. 95:1055–
820 1072.

821 Nguyen L.-T., Schmidt H.A., von Haeseler A., Minh B.Q. 2015. IQ-TREE: a fast and
822 effective stochastic algorithm for estimating maximum-likelihood phylogenies. *Mol. Biol.*
823 *Evol*. 32:268–274.

824 Nosil P. 2008. Speciation with gene flow could be common. *Mol Ecol*. 17:2103-2106.

825 Oliver J.C. 2013. Microevolutionary processes generate phylogenomic discordance at ancient
826 divergences. *Evolution*. 67:1823–1830.

827 Ortiz, E.M. 2019. vcf2phylip v2.0: convert a VCF matrix into several matrix formats for
828 phylogenetic analysis. DOI:10.5281/zenodo.2540861

829 Pham K. K., Hipp A. L., Manos P. S., & Cronn R. C. 2017. A time and a place for
830 everything: phylogenetic history and geography as joint predictors of oak plastome
831 phylogeny. *Genome*. *60*:720-732.

832 Parins-Fukuchi C., Stull G.W., Smith S.A. 2021. Phylogenomic conflict coincides with rapid
833 morphological innovation. *Proc. Natl. Acad. Sci*. 118:e2023058118.

834 Parvathi M.S., Nataraja K.N., Reddy Y.A., Naika M.B., Gowda M.V. 2019. Transcriptome
835 analysis of finger millet (Eleusine coracana (L.) Gaertn.) reveals unique drought responsive
836 genes. *J. Genet*. 98:1–12.

837 Paun, O., Turner, B., Trucchi, E., Munzinger, J., Chase, M. W., & Samuel, R. (2016).
838 Processes driving the adaptive radiation of a tropical tree (Diospyros, Ebenaceae) in New
839 Caledonia, a biodiversity hotspot. *Systematic Biology*, *65*(2), 212–227.
840 https://doi.org/10.1093/sysbio/syv076

841 Pease J.B., Brown J.W., Walker J.F., Hinchliff C.E., Smith S.A. 2018. Quartet Sampling
842 distinguishes lack of support from conflicting support in the green plant tree of life. *Am. J.*
843 *Bot*. 105:385–403.

844 Pease J.B., Haak D.C., Hahn M.W., Moyle L.C. 2016. Phylogenomics reveals three sources
845 of adaptive variation during a rapid radiation. *PLOS Biol*. 14:e1002379.

846 Pérez-Escobar O.A., Chomicki G., Condamine F.L., Karremans A.P., Bogarín D., Matzke
847 N.J., Silvestro D., Antonelli A. 2017. Recent origin and rapid speciation of Neotropical
848 orchids in the world's richest plant biodiversity hotspot. *New Phytol*. 215:891–905.

849 Picard Toolkit. 2018. Broad Institute, GitHub Repository:
850 http://broadinstitute.github.io/picard/. *Broad Institute*.

851 Pinzón J.P., Ramírez-Morillo I.M., Carnevali G., Barfuss M.H., Till W., Tun J., Ortiz-Díaz
852 J.J. 2016. Phylogenetics and evolution of the *Tillandsia utriculata* complex (Bromeliaceae,

853 Tillandsioideae) inferred from three plastid DNA markers and the ETS of the nuclear
854 ribosomal DNA. *Bot. J. Linn. Soc*. 181:362–390.

855 Poplin R., Ruano-Rubio V., DePristo M.A., Fennell T.J., Carneiro M.O., Auwera G.A.V. der,
856 Kling D.E., Gauthier L.D., Levy-Moonshine A., Roazen D., Shakir K., Thibault J., Chandran
857 S., Whelan C., Lek M., Gabriel S., Daly M.J., Neale B., MacArthur D.G., Banks E. 2018.
858 Scaling accurate genetic variant discovery to tens of thousands of samples. *BioRxiv*:201178.

859 Quinlan A.R., Hall I.M. 2010. BEDTools: a flexible suite of utilities for comparing genomic
860 features. *Bioinformatics*. 26:841–842.

861 R Core Team. 2020. R: A language and environment for statistical computing. *Vienna,*
862 *Austria: R Foundation for Statistical Computing*.

863 Renaud G., Stenzel U., Maricic T., Wiebe V., Kelso J. 2015. deML: robust demultiplexing of
864 Illumina sequences using a likelihood-based approach. *Bioinforma. Oxf. Engl*. 31:770–772.

865 Revell L.J. 2012. phytools: an R package for phylogenetic comparative biology (and other
866 things). *Methods Ecol. Evol*. 3:217–223.

867 Richardson J.E., Pennington R.T., Pennington T.D., Hollingsworth P.M. 2001. Rapid
868 diversification of a species-rich genus of Neotropical rain forest trees. *Science*. 293:2242–
869 2245.

870 Rivera N.L. 2019. *Exploring genomic relationships in Tillandsia subgenus Tillandsia*.
871 [Master‘s Thesis]. University of Vienna. htpps://doi.org/10.25365/thesis.57906

872 Rundell R.J., Price T.D. 2009. Adaptive radiation, nonadaptive radiation, ecological
873 speciation and nonecological speciation. *Trends Ecol. Evol*. 24:394–399.

874 Salichos L., Rokas A. 2013. Inferring ancient divergences requires genes with strong
875 phylogenetic signals. *Nature*. 497:327–331.

876 Sankararaman S., Mallick S., Dannemann M., Prüfer K., Kelso J., Pääbo S., Patterson N.,
877 Reich D. 2014. The genomic landscape of Neanderthal ancestry in present-day humans.
878 *Nature*. 507:354–357.

879 Schluter D. 2000. *The ecology of adaptive radiation*. OUP Oxford.

880 Seehausen O., Butlin R.K., Keller I., Wagner C.E., Boughman J.W., Hohenlohe P.A., Peichel
881 C.L., Saetre G.-P., Bank C., Brännström Å. 2014. Genomics and the origin of species. *Nat.*
882 *Rev. Genet*. 15:176–192.

883 Sistla S., Rao D.N. 2004. S-Adenosyl-L-methionine–dependent restriction enzymes. *Crit.*
884 *Rev. Biochem. Mol. Biol*. 39:1–19.

885 Slovak M., Melichárková A., Štubňová E.G., Kučera J., Mandáková T., Smyčka J., Lavergne
886 S., Passalacqua N.P., Vďačný P., Paun O. 2023. Pervasive introgression during rapid
887 diversification of the European mountain genus *Soldanella* (L.) (Primulaceae). *Syst. Biol.*
888 syac071. https://doi.org/10.1093/sysbio/syac071

889 Smith, L.B. & Downs, R.J. 1977. Tillandsioideae (Bromeliaceae). *Flora Neotrop*. 14:798-
890 800.

891 Smith S.A., Moore M.J., Brown J.W., Yang Y. 2015. Analysis of phylogenomic datasets
892 reveals conflict, concordance, and gene duplications with examples from animals and plants.
893 *BMC Evol. Biol*. 15:150.

894 Solís-Lemus C., Yang M., Ané C. 2016. Inconsistency of species tree methods under gene
895 flow. *Syst. Biol*. 65:843–851.

896 Soltis P.S., Folk R.A., Soltis D.E. 2019. Darwin review: angiosperm phylogeny and
897 evolutionary radiations. *Proc. R. Soc. B Biol. Sci*. 286:20190099.

898 Stankowski S., Chase M.A., Fuiten A.M., Rodrigues M.F., Ralph P.L., Streisfeld M.A. 2019.
899 Widespread selection and gene flow shape the genomic landscape during a radiation of
900 monkeyflowers. *PLoS Biol*. 17:e3000391.

Straub S.C.K., Moore M.J., Soltis P.S., Soltis D.E., Liston A., Livshultz T. 2014. Phylogenetic signal detection from an ancient rapid radiation: Effects of noise reduction, long-branch attraction, and model selection in crown clade Apocynaceae. *Mol. Phylogenet. Evol*. 80:169–185.

Stroud J.T., Losos J.B. 2016. Ecological opportunity and adaptive radiation. *Annu. Rev. Ecol. Evol. Syst*. 47:507–532.

Suarez-Gonzalez A., Lexer C., Cronk Q.C.B. 2018. Adaptive introgression: a plant perspective. *Biol. Lett*. 14:20170688.

Suh A., Smeds L., Ellegren H. 2015. The dynamics of incomplete lineage sorting across the ancient adaptive radiation of neoavian birds. *PLOS Biol*. 13:e1002224.

Suvorov A., Kim B.Y., Wang J., Armstrong E.E., Peede D., D'Agostino E.R.R., Price D.K., Waddell P.J., Lang M., Courtier-Orgogozo V., David J.R., Petrov D., Matute D.R., Schrider D.R., Comeault A.A. 2022. Widespread introgression across a phylogeny of 155 *Drosophila* genomes. *Curr. Biol*. 32:111-123.e5.

Taylor S.A., Larson E.L. 2019. Insights from genomes into the evolutionary importance and prevalence of hybridization in nature. *Nat. Ecol. Evol*. 3:170–177.

Than C., Ruths D., Nakhleh L. 2008. PhyloNet: a software package for analyzing and reconstructing reticulate evolutionary relationships. *BMC Bioinformatics*. 9:1–16.

Till W. 2000. *Tillandsioideae*. D.H. Benzing, ed. Bromeliaceae: profile of an adaptive radiation. New York, New York: Cambridge University Press. p. Pp. 555-571.

Vera-Paz S.I., Granados Mendoza C., Díaz Contreras Díaz D.D., Jost, M., Salazar, G.A., Rossado, A.J., Montes-Azcué, C.A., Hernández-Gutiérrez, R., Magallon, S., Sánchez-González, L.A., Gouda, E.J., Cabrera L.I., Ramírez-Morillo, I.M., Flores-Cruz, M., Granados-Aguilar, X., Martínez-García, A.L., Hornung-Leoni, C.T.,Michael H.J. Barfuss, M.H.J., Wanke, S. 2023. Plastome phylogenomics reveals an early Pliocene North-and Central America colonization by long-distance dispersal from South America of a highly diverse bromeliad lineage. Front. Plant Sci. 14:1205511.

Victoriano-Romero E., Valencia-Díaz S., Toledo-Hernández V. H., Flores-Palacio, A. 2017. Dispersal limitation of *Tillandsia* species correlates with rain and host structure in a central Mexican tropical dry forest. *PloS one*, *12*:2.

Wang L.-G., Lam T.T.-Y., Xu S., Dai Z., Zhou L., Feng T., Guo P., Dunn C.W., Jones B.R., Bradley T., Zhu H., Guan Y., Jiang Y., Yu G. 2020. Treeio: an R package for phylogenetic tree input and output with richly annotated and associated data. *Mol. Biol. Evol*. 37:599–603.

934 Wendel J.F., Doyle J.J. 1998. Phylogenetic incongruence: Window into genome history and
935 molecular evolution. In: Soltis D.E., Soltis P.S., Doyle J.J., editors. Molecular systematics of
936 plants II: DNA sequencing. Springer US: pp. 265– 296.

937 Whitfield J.B., Lockhart P.J. 2007. Deciphering ancient rapid radiations. *Trends Ecol*. Evol.
938 22:258–265.

939 Winkler S. 1990. Zur Evolution der Gattung *Tillandsia* L. Bot. Jahrb. Syst. 112:43–77.

940 Wogan G.O.U., Yuan M.L., Mahler D.L., Wang I.J. 2023 Hybridization and transgressive
941 evolution generate diversity in an adaptive radiation of Anolis lizards. *Syst. Biol*. syad026.

942 Wong, E. L., Hiscock, S. J., & Filatov, D. A. 2022. The role of interspecific hybridisation in
943 adaptation and speciation: Insights from studies in Senecio. *Front. Plant Sci*. 13:907363.

944 Yan H., Jiang J. 2007. Rice as a model for centromere and heterochromatin research.
945 *Chromosome Res*. 15:77–84.

946 Yardeni G., Viruel J., Paris M., Hess J., Groot Crego C., de La Harpe M., Rivera N., Barfuss
947 M.H.J., Till W., Guzmán-Jacob V., Krömer T., Lexer C., Paun O., Leroy T. 2022. Taxon-
948 specific or universal? Using target capture to study the evolutionary history of rapid
949 radiations. *Mol. Ecol. Resour*. 22:927–945.

950 Yu G. 2020. Using ggtree to visualize data on tree-like structures. *Curr. Protoc. Bioinforma*.
951 69:e96.

952 Yu Y., Nakhleh L. 2015. A maximum pseudo-likelihood approach for phylogenetic networks.
953 *BMC Genomics*. 16:S10.

954 Zeberg H., Pääbo S. 2020. The major genetic risk factor for severe COVID-19 is inherited
955 from Neanderthals. *Nature*. 597:610–612.

956 Zhang C., Rabiee M., Sayyari E., Mirarab S. 2018. ASTRAL-III: polynomial time species
957 tree reconstruction from partially resolved gene trees. *BMC Bioinformatics*. 19:153.

958 Zhang D., Rheindt F.E., She H., Cheng Y., Song G., Jia C., Qu Y., Alström P., Lei F. 2021.
959 Most genomic loci misrepresent the phylogeny of an avian radiation because of ancient gene
960 flow. *Syst. Biol*. 70:961–975.

961 Zheng X., Levine D., Shen J., Gogarten S.M., Laurie C., Weir B.S. 2012. A high-
962 performance computing toolset for relatedness and principal component analysis of SNP data.
963 *Bioinformatics*. 28:3326–3328.

964 **Figures**

965 **Figure 1.** Coalescent-based species trees generated on 3,785 genomic windows with
966 ASTRAL-III for 64 individuals representing 34 species of *Tillandsia* subg. *Tillandsia*, plus
967 two outgroups. Branch lengths are given in coalescent units. Node values represent local
968 posterior probabilities for the main topology and are equal to one unless noted otherwise. Pie
969 charts at the nodes show levels of gene tree discordance: the percentages of concordant gene
970 trees (blue), the top alternative bipartition (green), other conflicting topologies (red) and
971 uninformative gene trees (grey).

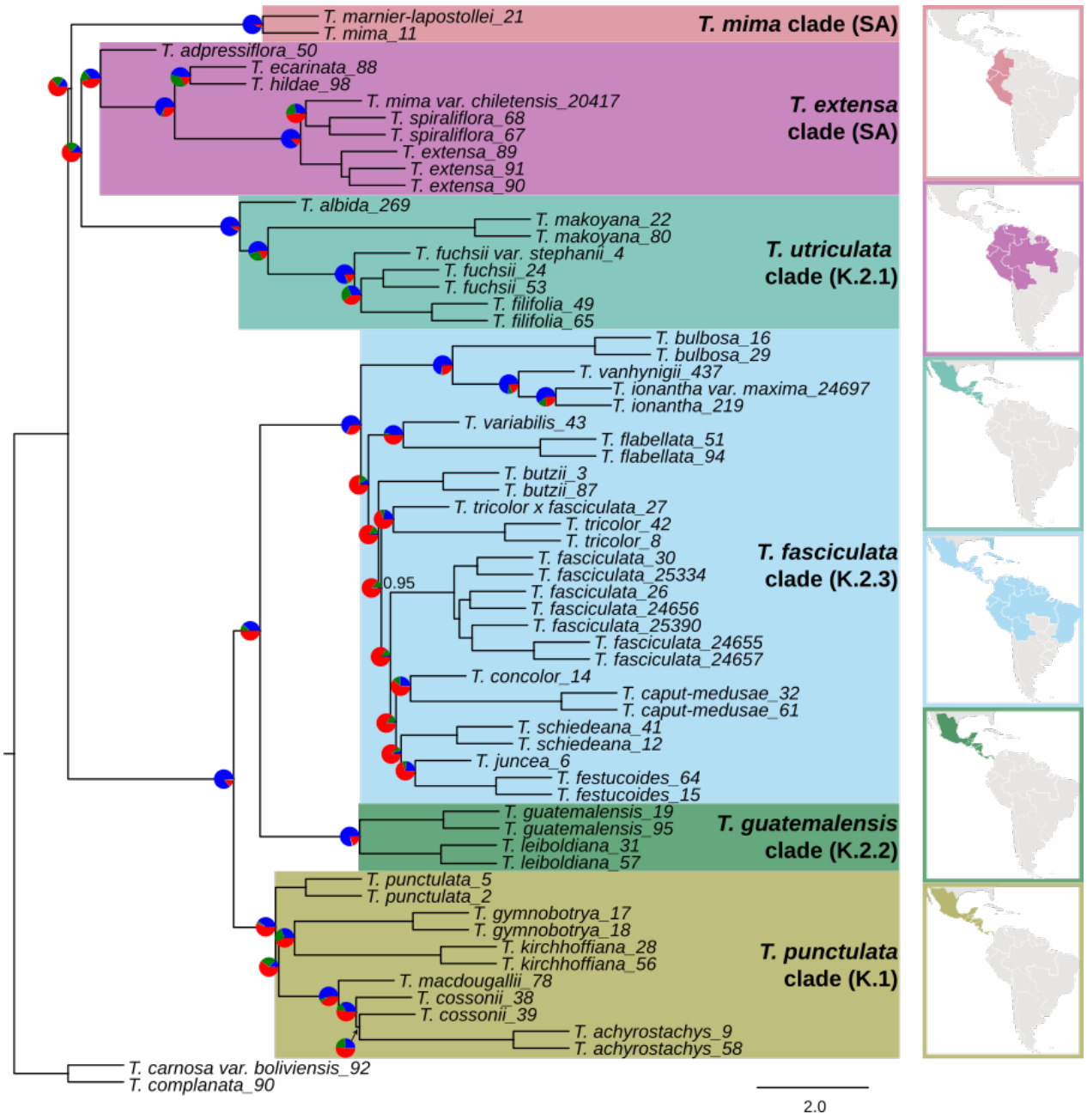

Figure 2. Heatmap summarizing 7,141 four-taxon D-statistic tests. *Tillandsia complanata* was used as the outgroup in all tests. The four taxa in each test have been rearranged to always obtain positive D values and P2 and P3 are shown on the axes. Colour indicates the value of D and the log value of p-value, the latter estimated using a block jackknife procedure with a 200kb window size and corrected for family-wise error rate. Colours on the bars correspond to the clades in Figure 1.

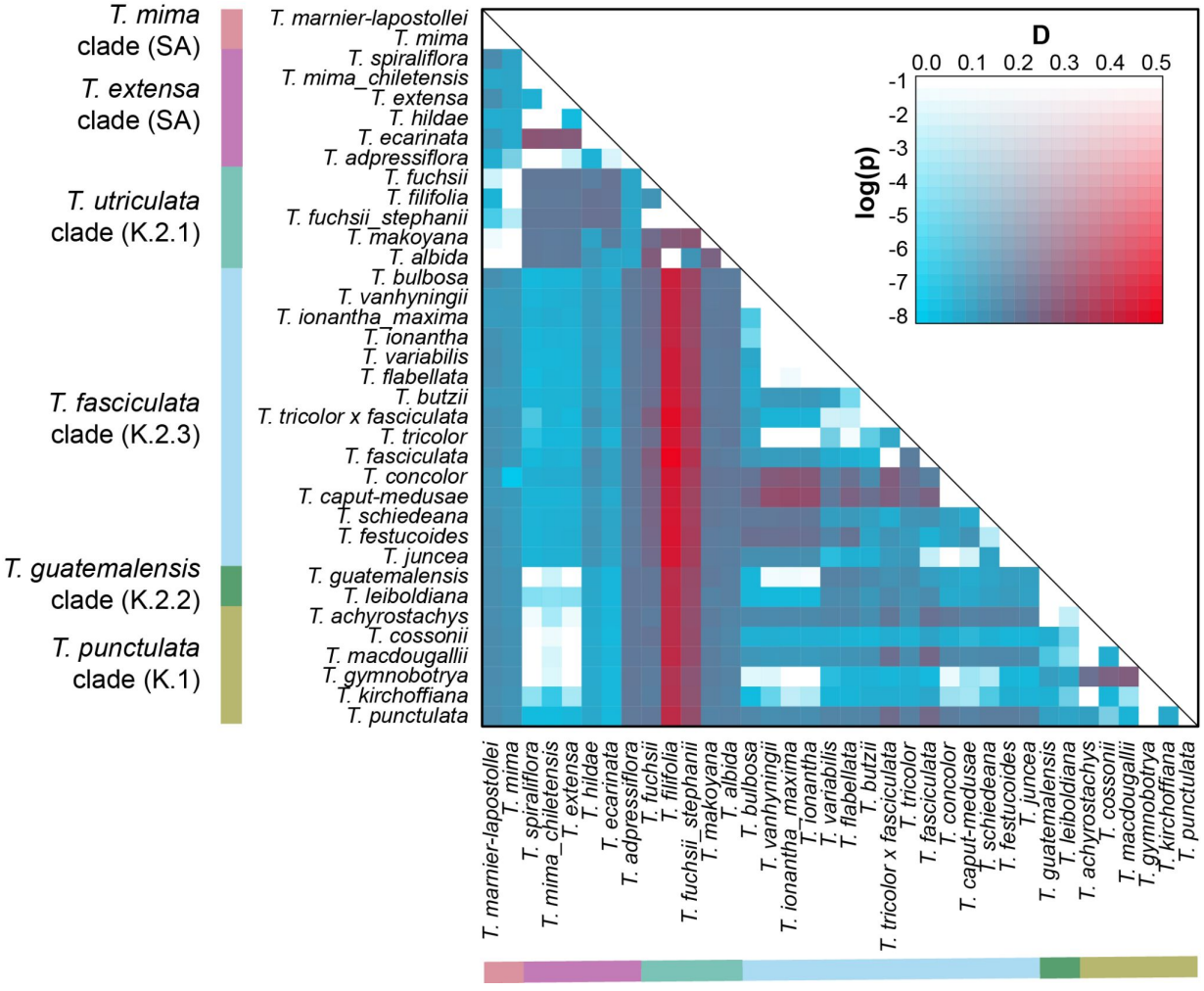

Figure 3. Heatmap summarising the statistic $f_b(C)$, where excess sharing of derived alleles is inferred between the branch of the tree on the Y axis and the species C on the X axis. The ASTRAL species tree was used as input topology for the branch statistic. The matrix is colored according to the legend of the $f_b(C)$ values and grey squares correspond to tests that are inconsistent with the ASTRAL phylogeny. Dots within the matrix denote a significant p-value, estimated using a block jackknife procedure and corrected for family wise error rate. Colours correspond to the clades in Figure 1.

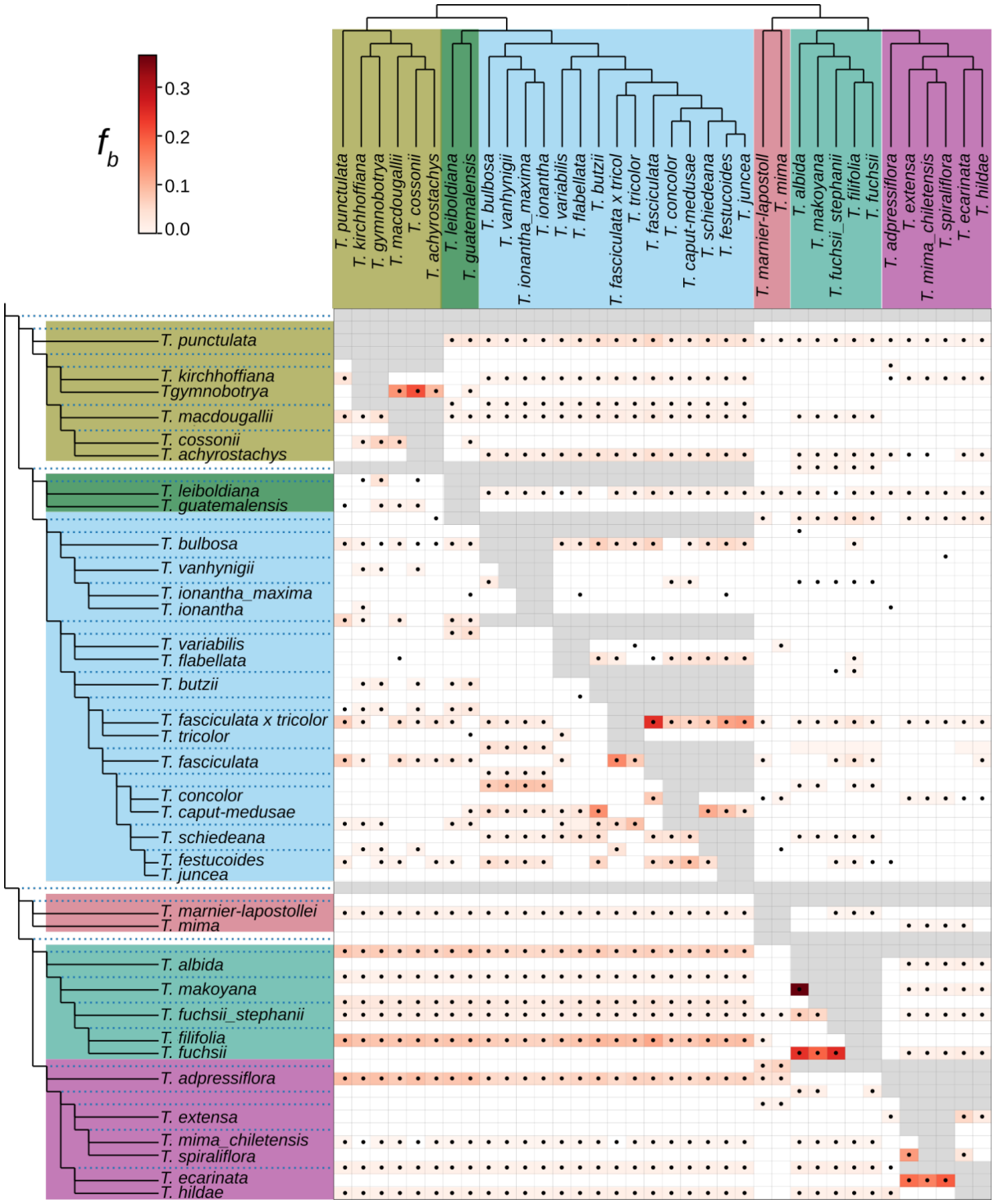

985 **Figure 4.** Best maximum pseudo-likelihood species networks inferred with PhyloNet for zero
986 to three reticulation events. Curved branches indicate reticulation events. Numbers next to
987 curved branches indicate inheritance probabilities for each event. Colours correspond to the
988 clades in Figure 1.

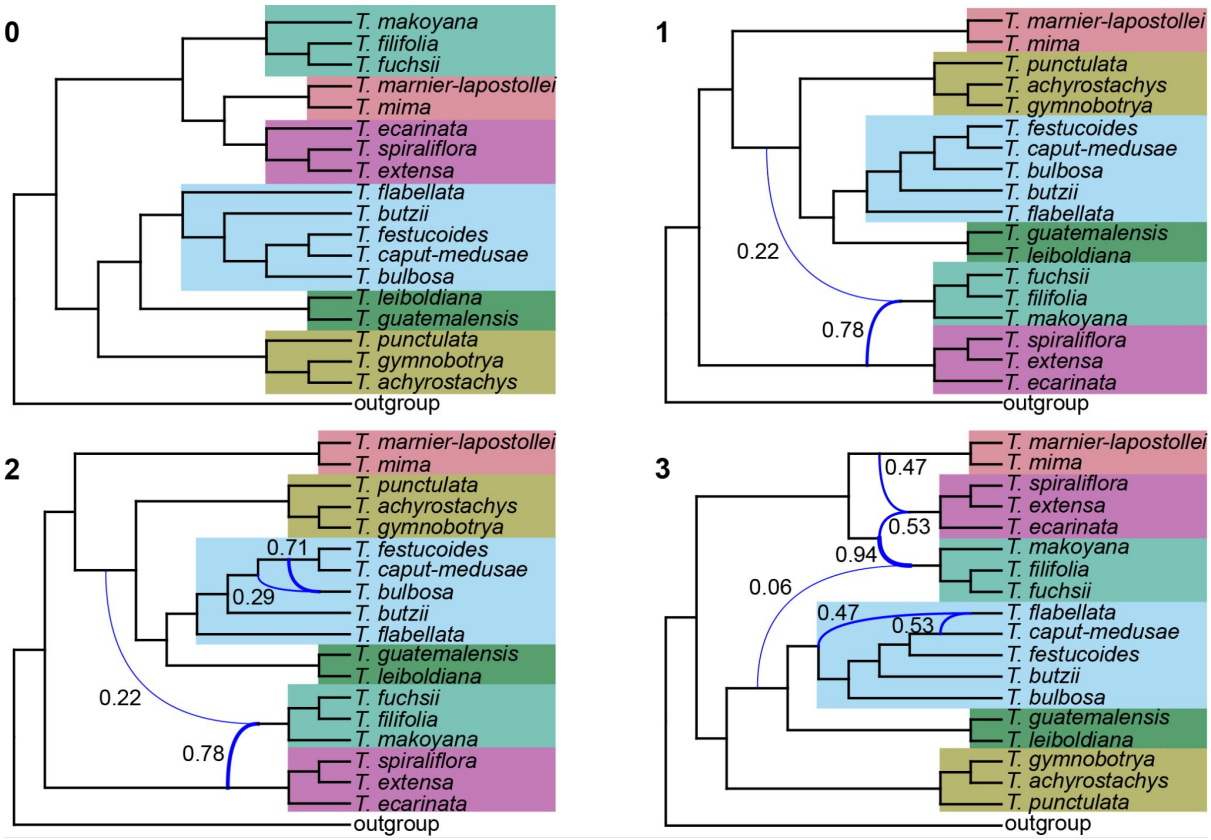

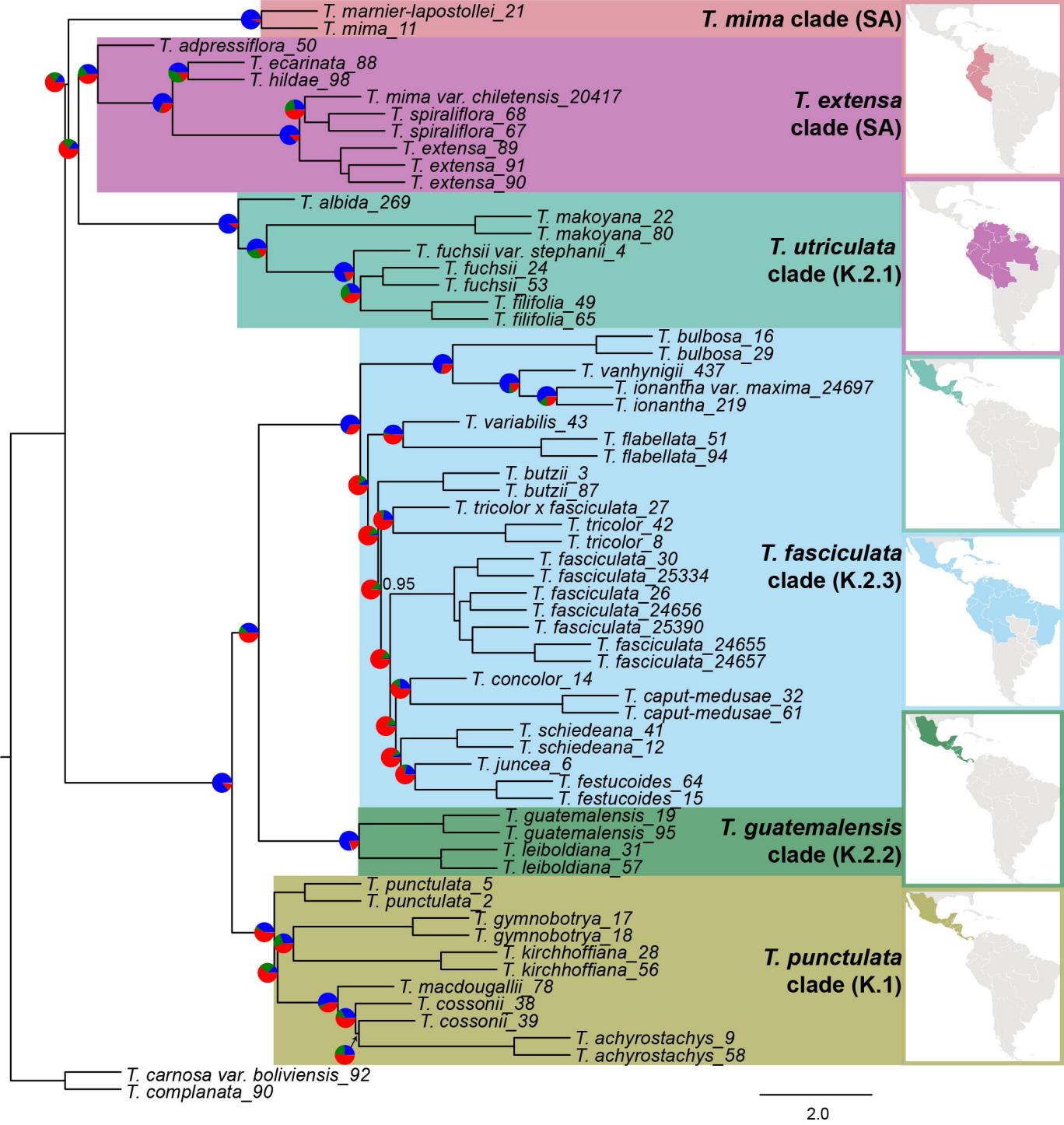
T. marnier-lapostollei_21
T. mima_11
T. mima clade (SA)
T. adpressiflora_50
T. ecarinata_88
T. hildae_98
T. mima var. chiletensis_20417
T. spiraliflora_68
T. spiraliflora_67
T. extensa_89
T. extensa_91
T. extensa_90
T. extensa clade (SA)
T. albida_269
T. makoyana_22
T. makoyana_80
T. fuchsii var. stephanii_4
T. fuchsii_24
T. fuchsii_53
T. filifolia_49
T. filifolia_65
T. utriculata clade (K.2.1)
T. bulbosa_16
T. bulbosa_29
T. vanhynigii_437
T. ionantha var. maxima_24697
T. ionantha_219
T. variabilis_43
T. flabellata_51
T. flabellata_94
T. butzii_3
T. butzii_87
T. tricolor x fasciculata_27
T. tricolor_42
T. tricolor_8
T. fasciculata_30
T. fasciculata_25334
0.95
T. fasciculata_26
T. fasciculata_24656
T. fasciculata_25390
T. fasciculata_24655
T. fasciculata_24657
T. concolor_14
T. caput-medusae_32
T. caput-medusae_61
T. schiedeana_41
T. schiedeana_12
T. juncea_6
T. festucoides_64
T. festucoides_15
T. fasciculata clade (K.2.3)
T. guatemalensis_19
T. guatemalensis_95
T. leiboldiana_31
T. leiboldiana_57
T. guatemalensis clade (K.2.2)
T. punctulata_5
T. punctulata_2
T. gymnobotrya_17
T. gymnobotrya_18
T. kirchhoffiana_28
T. kirchhoffiana_56
T. macdougallii_78
T. cossonii_38
T. cossonii_39
T. achyrostachys_9
T. achyrostachys_58
T. punctulata clade (K.1)
T. carnosa var. boliviensis_92
T. complanata_90
2.0

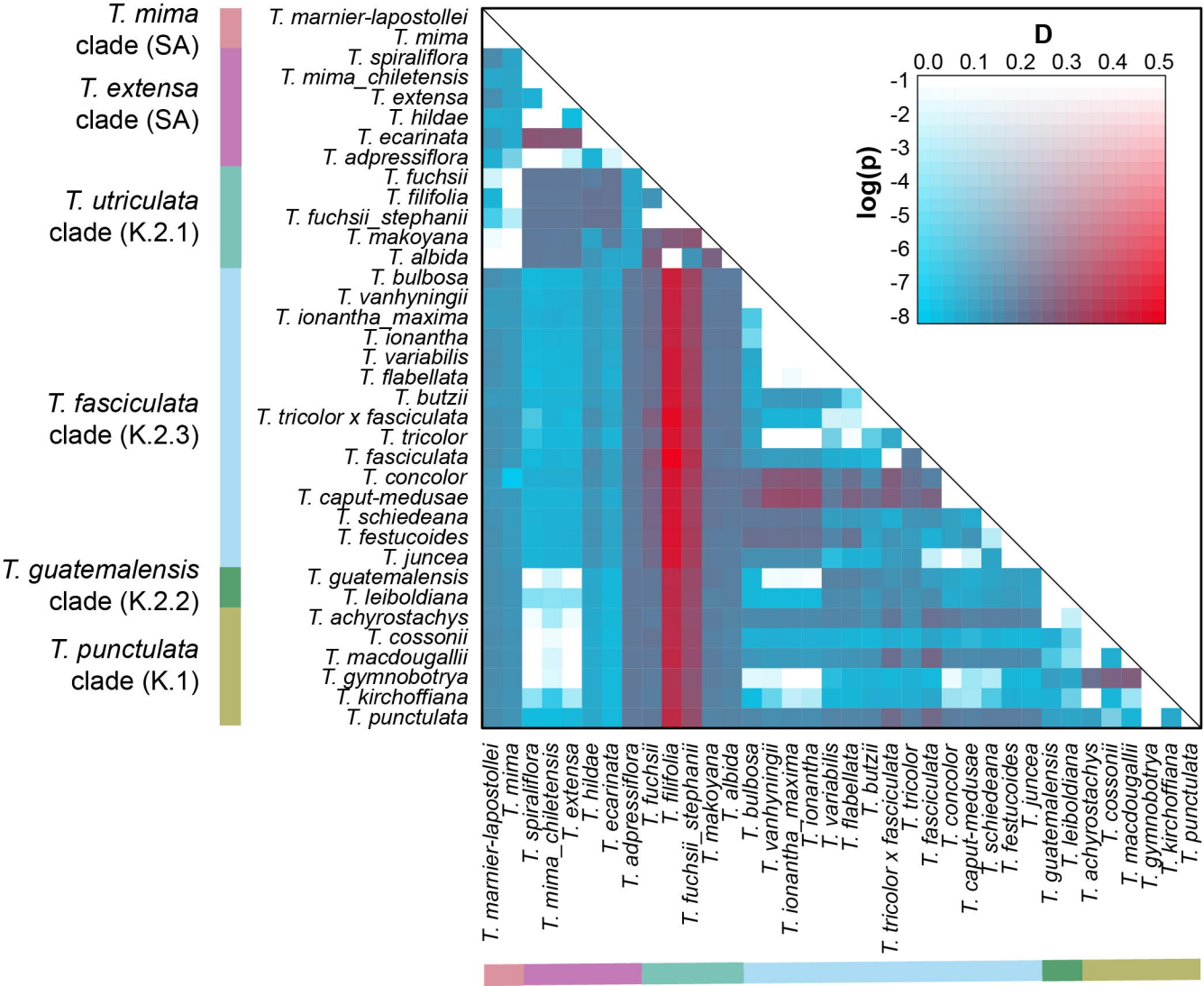
T. mima clade (SA)
T. extensa clade (SA)
T. utriculata clade (K.2.1)
T. fasciculata clade (K.2.3)
T. guatemalensis clade (K.2.2)
T. punctulata clade (K.1)
T. marnier-lapostollei
T. mima
T. spiraliflora
T. mima_chiletensis
T. extensa
T. hildae
T. ecarinata
T. adpressiflora
T. fuchsii
T. filifolia
T. fuchsii_stephanii
T. makoyana
T. albida
T. bulbosa
T. vanhyningii
T. ionantha_maxima
T. ionantha
T. variabilis
T. flabellata
T. butzii
T. tricolor x fasciculata
T. tricolor
T. fasciculata
T. concolor
T. caput-medusae
T. schiedeana
T. festucoides
T. juncea
T. guatemalensis
T. leiboldiana
T. achyrostachys
T. cossonii
T. macdougallii
T. gymnobotrya
T. kirchoffiana
T. punctulata
D
0.0 0.1 0.2 0.3 0.4 0.5
log(p)
-1 -2 -3 -4 -5 -6 -7 -8

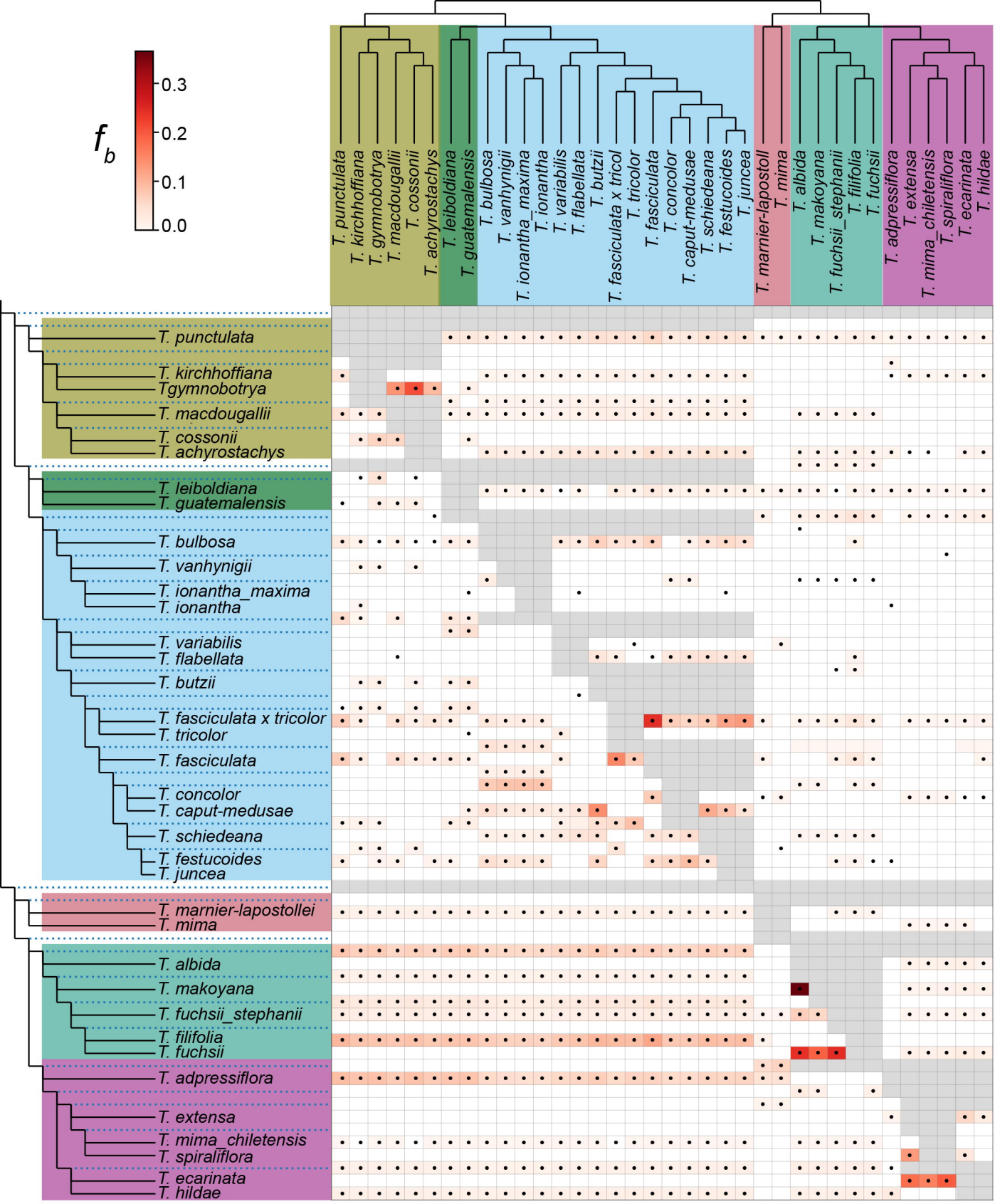
f_b
0.3
0.2
0.1
0.0
T. punctulata
T. kirchhoffiana
T. gymnobotrya
T. macdougallii
T. cossonii
T. achyrostachys
T. leiboldiana
T. guatemalensis
T. bulbosa
T. vanhynigii
T. ionantha_maxima
T. ionantha
T. variabilis
T. flabellata
T. butzii
T. fasciculata x tricol
T. tricolor
T. fasciculata
T. concolor
T. caput-medusae
T. schiedeana
T. festucoides
T. juncea
T. marnier-lapostoll
T. mima
T. albida
T. makoyana
T. fuchsii_stephanii
T. filifolia
T. fuchsii
T. adpressiflora
T. extensa
T. mima_chiletensis
T. spiraliflora
T. ecarinata
T. hildae

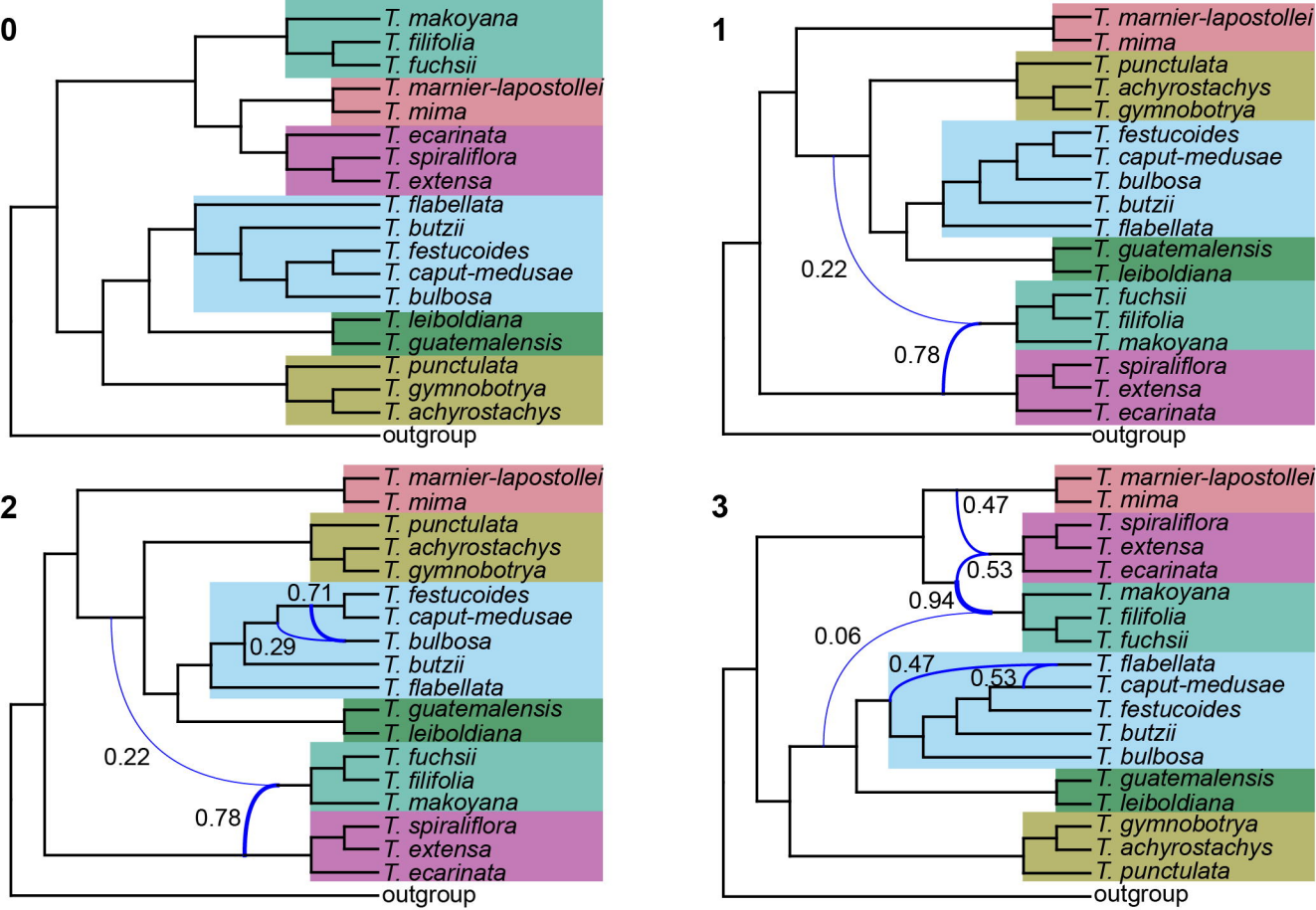
0
T. makoyana
T. filifolia
T. fuchsii
T. marnier-lapostollei
T. mima
T. ecarinata
T. spiraliflora
T. extensa
T. flabellata
T. butzii
T. festucoides
T. caput-medusae
T. bulbosa
T. leiboldiana
T. guatemalensis
T. punctulata
T. gymnobotrya
T. achyrostachys
outgroup
1
T. marnier-lapostollei
T. mima
T. punctulata
T. achyrostachys
T. gymnobotrya
T. festucoides
T. caput-medusae
T. bulbosa
T. butzii
T. flabellata
T. guatemalensis
T. leiboldiana
0.22
T. fuchsii
T. filifolia
T. makoyana
0.78
T. spiraliflora
T. extensa
T. ecarinata
outgroup
2
T. marnier-lapostollei
T. mima
T. punctulata
T. achyrostachys
T. gymnobotrya
0.71
T. festucoides
T. caput-medusae
0.29
T. bulbosa
T. butzii
T. flabellata
T. guatemalensis
T. leiboldiana
0.22
T. fuchsii
T. filifolia
T. makoyana
0.78
T. spiraliflora
T. extensa
T. ecarinata
outgroup
3
T. marnier-lapostollei
T. mima
0.47
T. spiraliflora
T. extensa
0.53
T. ecarinata
0.94
T. makoyana
T. filifolia
0.06
T. fuchsii
0.47
T. flabellata
0.53
T. caput-medusae
T. festucoides
T. butzii
T. bulbosa
T. guatemalensis
T. leiboldiana
T. gymnobotrya
T. achyrostachys
T. punctulata
outgroup